VERMONT GEOLOGY

MARCH 2001 VOLUME 8

FIELD TRIP GUIDEBOOK NUMBER 4

Field Guide for the Upper Monkton Formation in the Burlington Area

Charlotte J. Mehrtens

The Champlain Thrust Fault, Lone Rock Point, Burlington, Vermont

Rolfe S. Stanley

Faults and Fluids: The Vermont Foreland and Western Hinterland

Rolfe S. Stanley, Tracy Rushmer, Caleb Holyoke III, and Andrea Lini

Guide to Field Trips during the March 2001 Meeting, Northeastern Section, Geological Society of America
Vermont Geological Society
Editor: Stephen F. Wright

VERMONT GEOLOGY

Volume 8

FIELD TRIP GUIDEBOOK NUMBER 4

Guide to Field Trips Associated with the 2001 Northeastern Section Meeting of the Geological Society of America, Burlington, Vermont

March 11–14, 2001

Editor: Stephen F. Wright
Department of Geology
University of Vermont
Burlington, Vermont 05405

NOTE: Several of the field trip guides appearing in this issue of Vermont Geology are reprinted from other journals with the permission of the authors and the respective journals.

Additional copies of this guidebook and other publications of the Vermont Geological Society can be obtained by writing to:

Vermont Geological Society
% Department of Geology
University of Vermont
Burlington, Vermont 05405

Table of Contents

Note: The two field trip guides authored by Rolfe Stanley accompany the the field trip titled "The Stanley Outcrops" led by Barry Doolan and Keith Klepeis.

[1] Originally published as: Stanley, R.S., 1987, The Champlain thrust fault, Lone Rock Point, Burlington, Vermont; in Roy, D.C., ed., Geological Society of America Centennial Field Guide No. 5—Northeastern Section, p. 225–228.

[2] Originally published as: Stanley, R., Rushmer, T., Holyoke III, C., and Lini, A., 1999, Faults and Fluids: The Vermont Foreland and Western Hinterland; in Wright, S.F., ed., New England Intercollegiate Geological Conference Guidebook Number 91, p. 135–158.

Dedication

In Memory of

Rolfe S. Stanley

Professor of Geology
University of Vermont

The bedrock outcrops described in this guidebook are outdoor laboratories developed by Rolfe Stanley for generations of Vermont students. Each of Rolfe's classes has wrung new information and nuances from the outcrops, which further allowed Rolfe to apply his unique insight and enthusiasm for teachig observationsl skills in the field. These stops and others which comprise the "Stanley Outcrops" remain as fixtures to the geology curricula of UVM students. They are prize outcrops whose preservation will assure that future generations will gain new perspectives of Vermont geology.

Barry Doolan

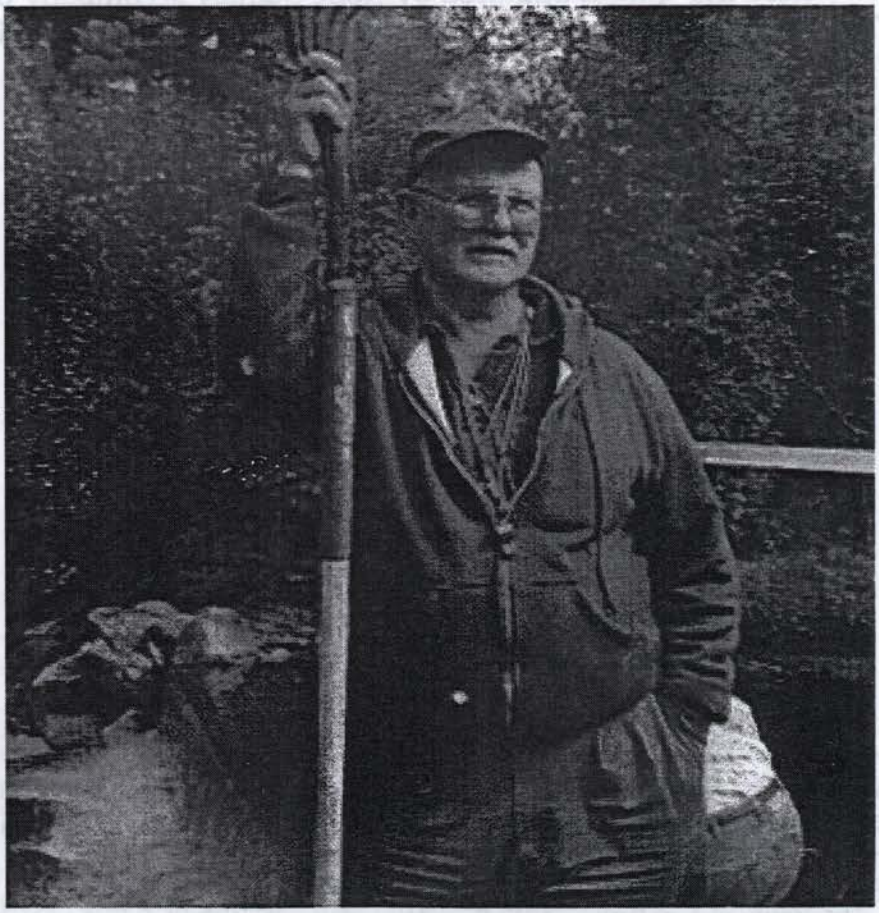

Rolfe at Warner Power Plant, NEIGC 1999.

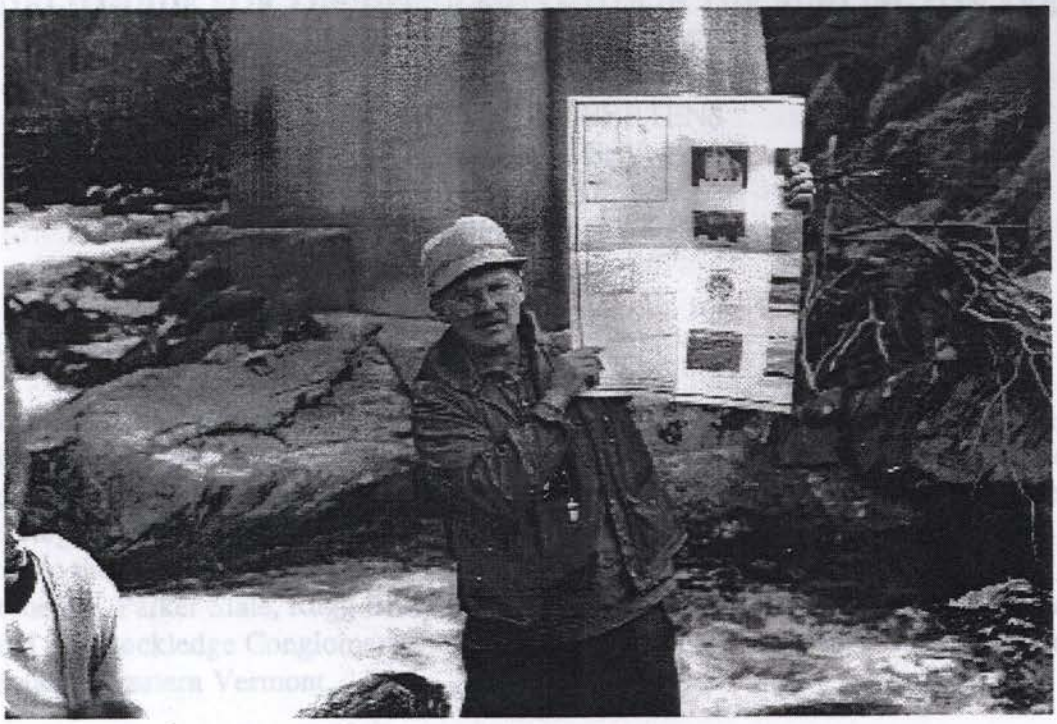

Rolfe at home in the field. Crash Bridge, NEIGC 1987.

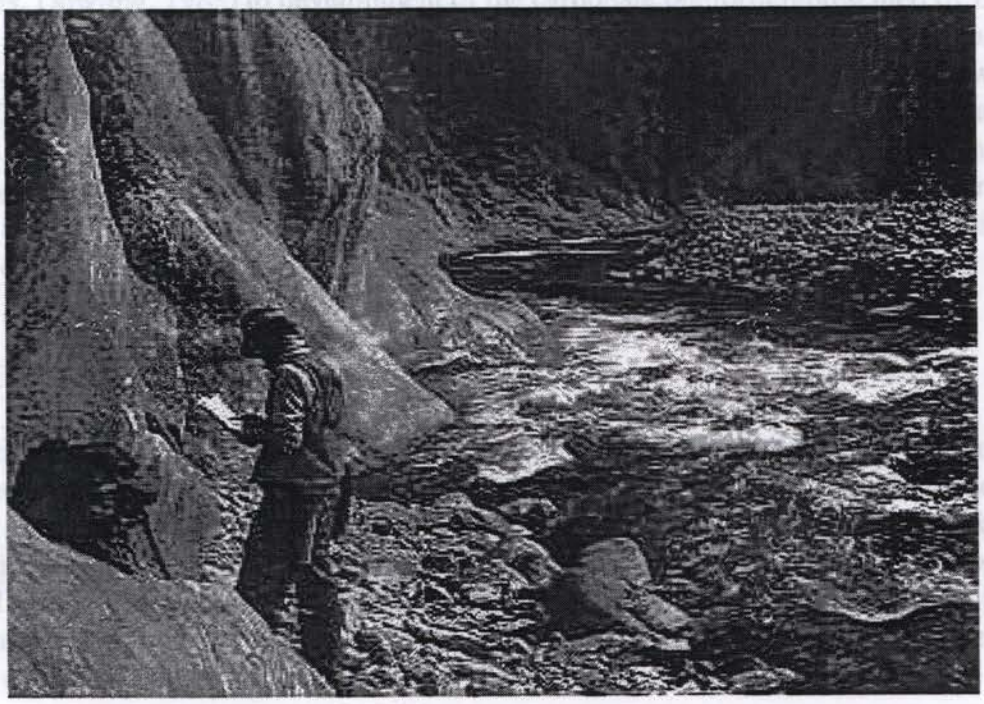

Rolfe in Taiwan.

FIELD GUIDE FOR THE UPPER MONKTON IN THE BURLINGTON AREA NEGSA, BURLINGTON, VT MARCH 12-14, 2001

CHARLOTTE MEHRTENS
Department of Geology
University of Vermont
Burlington, Vermont 05405

INTRODUCTION

The Cambro-Ordovician stratigraphic sequence in western Vermont consists of alternating siliciclastic (Cheshire, Monkton, Danby) and carbonate (Dunham, Winooski and Clarendon Springs) units which accumulated on a passively subsiding continental margin of the Iapetus Ocean (Rogers, 1968). These units, recording deposition in shallow water environments, are bordered to the east and north by deeper water basinal shale and breccia deposits (Parker Conglomerate, Parker Slate, Rugg Brook Conglomerate, Saxe Brook Dolomite, Skeels Corner Slate and and Rockledge Conglomerate). Figure 1 presents the stratigraphy of the Cambro-Ordovician in western Vermont.

Previous studies have described the sedimentology and stratigraphy of the Cheshire and Dunham Formations (Myrow, 1983 and Gregory, 1984, respectively). In brief, the Cheshire is interpreted to represent the transition from rift valley sedimentation (Pinnacle and Farfield Pond Formations, Dowling, 1988) to development of the carbonate platform represented by the overlying Dunham Dolomite. Studies of the Monkton Formation are much fewer in number. Goldberg and Mehrtens (1998) described the sedimentology and stratigraphy of the lower portion of the Monkton in which they documented an unconformity between the Dunham and Monkton, and basal Monkton non-marine facies. The upper portion of the Monkton has previously been described and interpreted to represent marine deposition within the peritidal (Rahmanian, 1981). Representative horizons of these environments are the focus of this field trip.

STRATIGRAPHY

The thickness of the Monkton at its type locality in western Vermont has been measured at 240 meters (Cady, 1945), however this represents the red-colored upper Monkton facies only. Goldberg and Mehrtens (1998) estimate that the lower, non-marine Monkton exposed in central Vermont includes a minimum of 50 meters, and potentially as much as as 150 meters of additional, not-exposed section. In the Burlington area, the upper Monkton is estimated to be approximately 330 meters thick, of which the upper 40 meters are exposed between the two field trip stops described here.

The nature of the lower contact of the Monkton with the Dunham varies geographically. Goldberg and Mehrtens (1998) describe the basal beds of Monkton as silty dolostones overlying

the Dunham's buff-colored dolostone in the Salisbury region (south and east of Middlebury), which when palinspastically restored, represent the most eastward, down-dip Monkton localities yet studied. In the Middlebury area, they describe the contact as an erosional unconformity between the carbonate clast-rich Monkton silty dolostones and the Dunham Dolostone. No karst surfaces were identified here, but a karst origin for the clasts at the top of the Monkton to the north has been suggested. Welby (1961) described the Dunham and Monkton contact as difficult to distinguish when the basal bed of Monkton was not a quartzite. He defined the base of the Monkton as the lowest quartzite bed over one foot in thickness that is separated by less than 25 feet of dolostone.

The contact of the Monkton with the overlying Winooski Dolomite is well exposed in the Burlington area and is described (Mehrtens, unpub) as occurring over an interval of approximately 10 meters, where red sand and siltstone horizons become progressively thinner and more widely spaced between dolostone horizons. The base of the Winooski is defined as occurring above the highest red-colored siliciclastic layer. Although difficult to arrange to visit, the above stratigraphy is very well exposed at Whitcomb's Quarry, Winooski.

BIOSTRATIGRAPHY

Shaw (1962) identified six species of trilobites from Monkton Quartzite and Parker Shale outcrops in northwestern Vermont, which were dated as Lower Cambrian in age. From this evidence, Shaw concluded that the Parker represented the offshore, deeper-water equivalent of the Monkton. With few exceptions fossils are uncommon in the Cambrian shelf units in general, making biostratigraphic correlation between the shelf and basin environments difficult. However, the basinal deposits have yielded a diverse fauna, enabling a fairly complete biostratigraphic subdivision of the Cambro-Ordovician shales in western Vermont (see Figure 3). Correlation between the basinal and shelf units has therefore been based on physical stratigraphy based on detailed mapping, which documents interfingering, and petrographic studies, which document provenance, (see Mehrtens and Dorsey, 1987; Mehrtens and Borre, 1989, Mehrtens and Hadley, 1995). These studies have documented correlations between the Monkton and the lower Parker Slate and Rugg Brook Conglomerate.

The trilobite faunas described by Shaw (1962) were used by Palmer and James (1979) to correlate the Monkton to other Lower Cambrian units in the Appalachians. The Monkton is correlated to the Rome, Waynesboro and Hawke Bay Formations from the southern through northern Appalachians (Figure 2). Most importantly, they recognized that the Monkton Quartizte is the regressive sandstone deposit correlative to an unconformity with the adjacent basinal sediments (the Parker Slate), which they interpreted to represent a regression along the entire Iapetus margin. They termed this unconformity the "Hawke Bay Event", which represents the absence of basinal sediment accumulation spanning from the top of the *Bonnia-Olenellus* (Lower Cambrian) to the top of the *Bathyuriscus-Elrathina* Zones (late Middle Cambrian). During this hiatus, regressive sandstones were deposited on the adjacent shelves flanking the Iapetus.

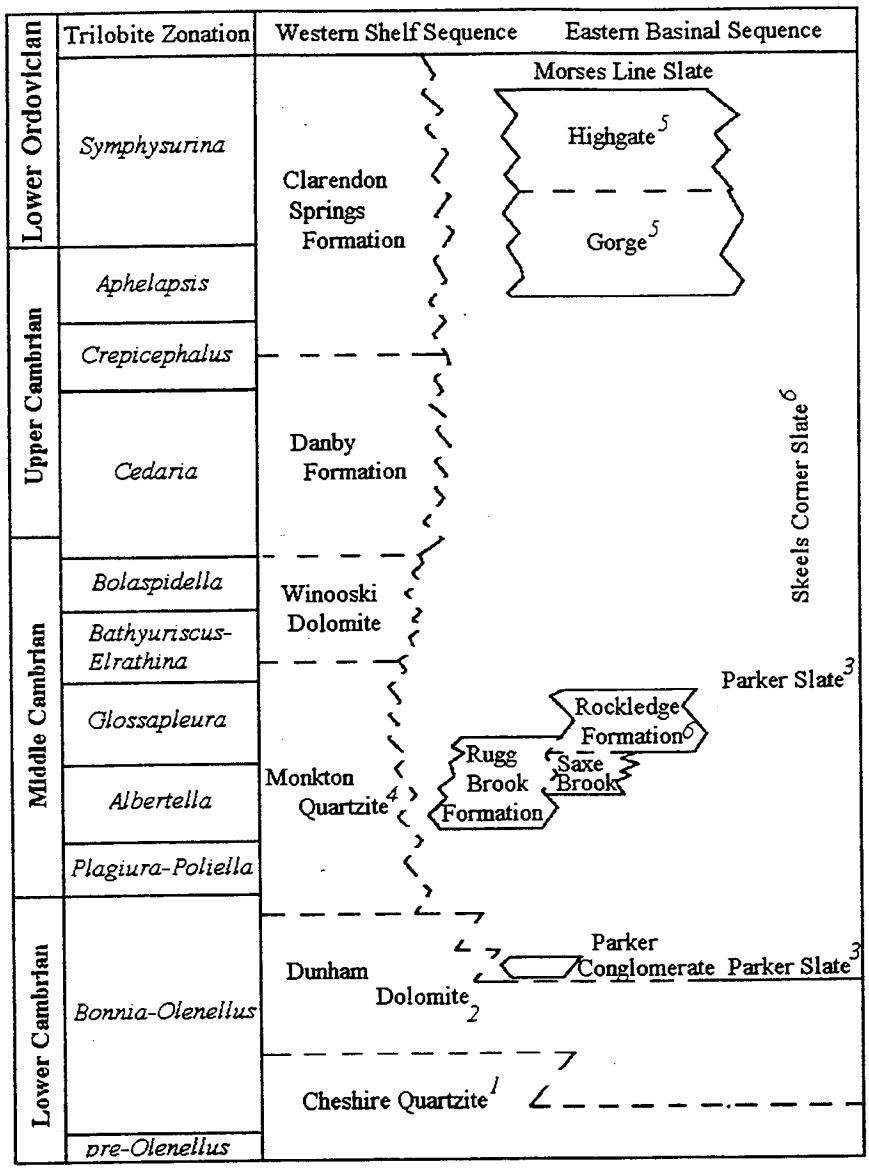

Figure 1. Correlation chart for the Cambrian and Lower Ordovician shelf and basinal sequences for northwestern Vermont. Where faunal control exists the unit is labeled with a number that corresponds to: #1, Walcott, 1886, #2, Mehrtens and Gregory, 1984, #3, Palmer, 1971, #4, Schuchert 1933 and 1937, #5, Landing, 1983, #6, Shaw, 1958. From Hadley, 1991.

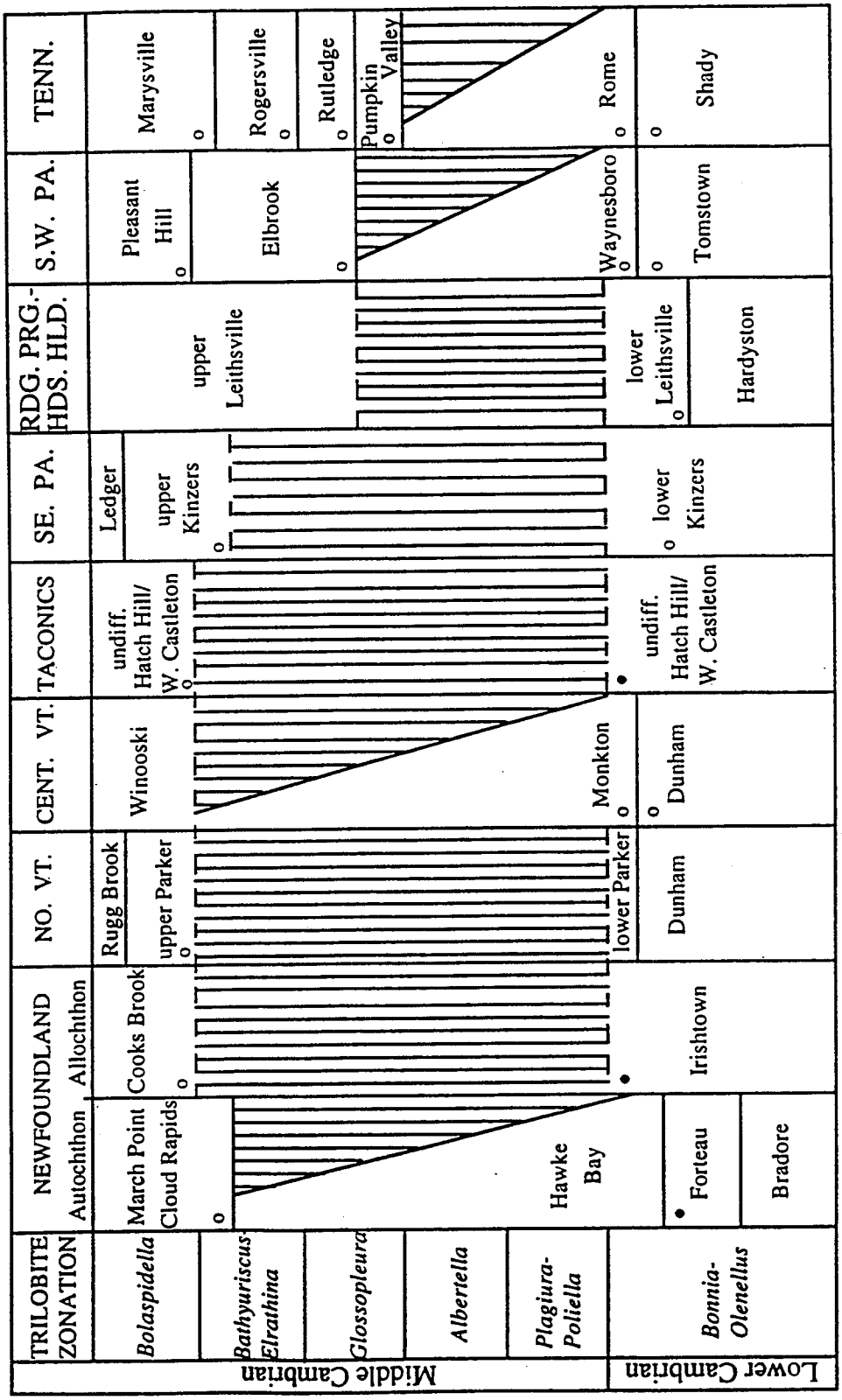

Figure 2. Biostratigraphic correlation chart for eastern North America. Small open circles indicate generalized faunal control. From Palmer and James (1980).

REGIONAL TRENDS

There are several important regional trends in the Monkton which bear on its paleoenvironmental interpretation. (1) As described in several State mapping reports, the Monkton pinches out in the Milton, Vermont area where it passes into the shelf edge and basinal deposits of the conglomeratic Rugg Brook Formation (Mehrtens and Hadley, 1995). Where the Monkton terminates it is a grey-colored, massively bedded, cross bedded sandstone interpreted as a complex of sublittoral sheet sands and sand bars. A good exposure of the subtidal facies below the Winooski Dolostone occurs along Route 2 west of Interstate 89. These horizons have yielded trilobite fragments identifiable as Olenellus. (2) Rahmanian (1981) noted that the peritidal and intertidal facies of the Monkton prograde across subtidal dolostones of the open platform from south to north along strike of the outcrop belt. Excellent exposures of the prograding red-colored peritidal facies can be seen along I-89 north of Exit 16. And, (3) as noted above, Goldberg and Mehrtens (1998) described the non-marine to marine transition within the Monkton in central Vermont.

From these regional trends we can reconstruct a depositional model of a carbonate platform characterized by an abrupt platform to basin transition succeeded in various locales by non-marine fluvial facies or sublittoral sheet sandstones. Prograding across this shelf are tidally-dominated red-colored sandstones, siltstones and shales of the upper Monkton.

SEQUENCE STRATIGRAPHY

In their study of the Monkton, Goldberg and Mehrtens (1998) presented an interpretation of the cycles within the Cambro-Ordovician rocks of Vermont as explainable within the model of fluctuating eustatic sea level. The application of the sequence stratigraphy paradigm has been extensive (see, for example, Van Wagoner and Bertram, 1995) however, certain structural and stratigraphic criteria must be met in order for this model to be applied to the interpretation of a sequence of rocks. Goldberg and Mehrtens (1998) discuss the relevancy of applying this model to the Cambro-Ordovician sequence in Vermont and suggest that a sufficient level of structural interpretation, biostratigraphic control, and lithofacies documentation and interpretation exists for sequence stratigraphy to be useful in understanding these stratal patterns. The assumptions that: (1) rate of sea floor subsidence remains constant; (2) sediment supply remains constant and (3) the trend of eustatic sea level change is curvilinear, approaching sinusoidal or resolvable into small sinusoidal curves, are all reasonable for this passive margin.

Reviewing the entire sequence stratigraphy model is beyond the scope of this field guide and the reader is referred to Vail, et al. (1977), Posamentier and Vail (1988) and Van Wagoner and Bertram (1990) for thorough presentations. Basically, a sequence is defined as the fundamental unit of sequence stratigraphy consisting of a "relatively conformable succession of genetically related strata bounded by unconformities and their correlative conformities" (Posamentier and Vail, 1988, p. 125). Sequences are recognized as highstand, lowstand and transgressive systems tracts. A systems tract is composed of one or more depositional systems defined by: (1) their bounding surfaces (type 1 or 2 unconformity or sequence boundary), (2)

position within a sequence, and (3) parasequence geometry. Sequence stratigraphy predicts that eustatic sea level changes will produce a predictable sequence of lowstand-transgressive-highstand systems tracts. Each systems tract is associated with some part of the eustatic curve.

Based on: (1) the nature of the contacts between siliciclastic and carbonate units; (2) the parasequence geometry within a unit; and (3) trends in base level, we can interpret the Cambrian strata in Vermont in terms of its sea level history. The Dunham Dolomite is interpreted to represent a Highstand Systems Tract (HST) on the basis of prograding parasequences in this unit, which thicken up section (reflecting an increase in accomodation space which accompanies high sea level stand). Following a sea level highstand, the sequence stratigraphy model would predict a sea level lowering, which would be recorded by an unconformity between the Dunham and overlying Monkton. This is, in fact, what outcrop exposures of the contact in the Middlebury region reveal: erosion and a marine (Dunham) to non-marine (lower Monkton) transition (= Type 1 sequence boundary). Following erosion of the Dunham shelf, the lower Monkton non-marine facies represent lowstand systems tract deposition, which is followed by marine deposition of the familiar red-colored upper Monkton (=transgressive systems tract). In a transgressive system tract the parasequence geometry should exhibit a thinning-upwards trend as accomodation space is progressively reduced (note that regressive sandstones are deposited during this time). This is the pattern seen when the shallowing-up cycles at Redstone Quarry and Salmon Hole are studied and compared to horizons lower in the Upper Monkton. The overlying Winooski Dolostone represents the next highstand systems tract.

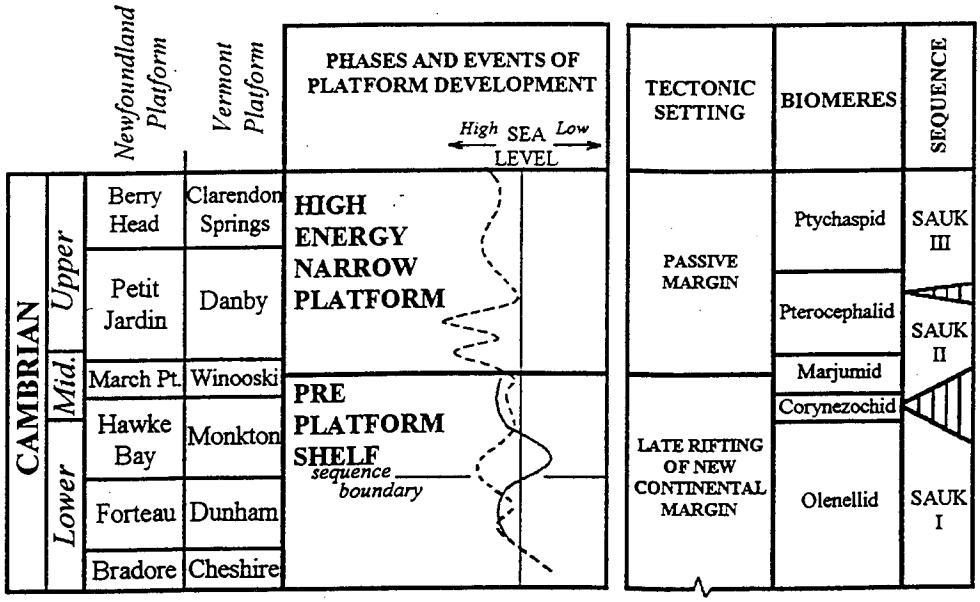

Figure 3. Modified sea level curve of James, et al. (1989) from Goldberg and Mehrtens (1998). The western Newfoundland curve is in dashed lines and the Vermont curve in solid lines. Where the two curves diverge (Monkton time) is interpreted to reflect local tectonic effects.

It was Palmer and James (1979) who first suggested that we should be able to distinguish between eustatic and local effects within the Hawke Bay Event. We think that this is the case. When comparing the sea level curve generated for Vermont to that of James, et al.'s (1989) sea level curve for the Cambro-Ordovician of Newfoundland, differences in base level between Newfoundland and Vermont are seen (figure 3). We have interpreted these differences to represent local effects, probably related to sediment supply (suggesting uplift of the Adirondacks). Petrographic analysis of the Monkton, especially its accessory mineral suite, suggests an Adirondack (Grenville gneiss) source for the sands.

The key to interpreting the sea level history of the entire Cambro-Ordovician margin lies, in great part, in understanding the smaller scale cycles, or parasequences, and these are very well exposed in the Burlington area and are the focus of this field trip.

LITHOFACIES DESCRIPTIONS

The upper Monkton is comprised of 6 lithofacies which occur in cyclic patterns.

Lithofacies 1: Buff-colored structureless dolostone

Description: This lithofacies is characterized by thick, structureless beds of dolostone that frequently contains quartz and feldspar grains disseminated throughout. The terrigenous material can increase in quantity to the point that the lithology becomes a sandy dolostone containing both planar laminations and ripples near the tops of these graded beds. Included within this lithofacies are also massive beds of dolostone which lack any terrigenous material.

Interpretation: This interpretation of the depositional environment of this lithofacies is extremely important when trying to interpret the architecture of the shallowing-up cycles characteristic of the upper Monkton Formation. Several lines of evidence suggest that this carbonate sediment was deposited in the shallwo peritidal or subtidal and did not accumulate in the supratidal: (1) Massive bedding characteristic of this lithofacies containing planar and cross laminated disseminated terrigenous material. (2) An absence of any evidence of subaerial exposure. (3) The overall abundance of dolostone within the Monkton. For example, the lowest horizons exposed at the Salmon Hole locality are 7 meters of massively bedded sandy dolostones; it is difficult to envision this quantity of material accumulating above fairweather or storm high tide line with no intervening terrigenous material. (4) Similarity to dolostone horizons recording the subtidal environment in both the underlying Dunham and overlying Winooski Formations. This dolostone is interpreted as the ambient background sediment into which the tidal flat sediments prograde.

Local Occurrence: This lithofacies is exposed at both Salmon Hole and Redstone Quarry.

Lithofacies 2: Cryptalgalaminite dolomite and shale horizons.

Description: The cryptalgalaminite horizons are orange-colored dolostones containing small rip-up clasts, dessication cracks, and vertical burrows. Red colored silt and shale accentuate the algal laminations. This lithofacies occurs as the caps to Lithofacies 5.

Interpretation: This lithofacies is interpreted to reflect deposition in the intertidal to supratidal setting.

Local Occurrence: This lithofacies is found at the Redstone Quarry locality.

Lithofacies 3: Rippled sandstone and shale

Description: This lithofacies consists of thin (1-3 cm) interbeds of fine to medium grained rippled sandstone (arkose to feldspathic litharenite in composition) draped with maroon-colored shale or shaley siltstone. Boudined beds of thin buff-colored dolostone can also be found interbedded with the above. Ripples are symmetrical, wave-generated, and interference varieties. Crestline trends are shown in Figures 4 and 5. Viewing the ripples in cross section reveals a complex internal structure of upward bundled laminations reflecting their wave origin. Many layers record the internal vertical sequence of planar laminations capped by ripples, a sequence which records emplacement under high velocity conditions with subsequent reworking. Beds laterally pinch out over several meters. Shale horizons exhibit mudcracks. Small vertical burrows are common and bedding plane exposures of rippled sands exhibit larger traces of the *Cruziana* inchnofacies.

Interpretation: There are many lines of evidence for an intertidal to shallow subtidal origin for this lithofacies with the mudcracks placing an upper limit on bathymetry. The abundance of planar laminations suggests that sediment was emplaced under high velocities and subsequently reworked by waves. Southard (personal communication) interpreted many of the ripples at Redstone Quarry as "dishpan ripples," implying extremely shallow water. The alternation of rippled sand and shale also reflects fluctuating velocities. Historically, (see, for example, Reineck and Singh, 1975) this has been the primary basis for interpreting a tidally-influenced origin to this type of couplet, and with the association with mudcracks here, is also the likely interpretation for this lithofacies.

Local Occurrence: This lithofacies makes up much of the Salmon Hole exposure and the lowest most horizons at Redstone Quarry

Lithofacies 4: Quartz Arenite

Description: This is a well-sorted, medium to coarse-grained white-to pink colored cross-bedded quartz arenite to subarkose. Because of the sorting, the cross beds can be difficult to see, however both tabular and trough cross beds occur, averaging 8 to 20 cm in height.

Interpretation: This lithofacies is interpreted to represent migrating megaripples. It's compositional and textural maturity is different from adjacent horizons and must be considered in any explanation for its origin. An offshore subtidal sand bar is one possible interpretation, with frequent wave action responsible for the sorting and cross bedding.

Local Occurrence: This lithofacies occurs only at the Redstone Quarry exposure.

Lithofacies 5: fine-medium grained red sandstone

Description: This is a dark red-colored fine-grained sandstone (sublitharenite to fledspathic litharenite in composition) which occurs in beds ranging from 8 to 30 cm in thickness. Its characteristic feature is the dewatering structures which occur thoughout.

Interpretation: The dewatering structures imply rapid deposition and the absence of any features of fluctuating velocity or subaerial exposure suggest a subtidal origin.

Local Occurrence: This lithofacies occurs at both Redstone Quarry and Salmon Hole.

Lithofacies 6: fine-to coarse-grained planar laminated sandstone
Description: This lithofacies is a fine to coarse-grained pink-colored planar laminated arkosic to subarkosic sandstone. Beds range from 1 to 4 cm in thickness. All beds exhibit graded bedding, some have several repeating fining-up cycles within them. Many beds also contain interference wave ripples, scoured bases and rip-up clasts.
Interpretation: Interpreting the structures within this facies suggests high velocity emplacement of sand, capable of scouring the substrate, followed by deceleration, frequently in pulses, and final reworking by waves. This is interpreted as a subtidal deposit, possibly emplaced from high velocity currents (storm enhanced?) followed by reworking within wave base.
Local Occurrence: This lithofacies is found at both Redstone Quarry and Salmon Hole.

CYCLES

Recognizing and interpreting the cycles within the upper Monkton is key to the Sequence Stratigraphy interpretation. In order to determine if cyclicity is present within the lower Monkton Goldberg and Mehrtens (1998) completed a Markov analysis to detect step-wise ordering (see Godin, 1991, for discussion of this procedure). This analysis confirmed the cyclicity of facies produced by fluvial channel bar formation. Harding (unpub. data) completed a Markov analysis of the upper Monkton in the Addison County area and Mehrtens (unpub. data) has done a Markov studies on the Monkton in the Burlington area. These studies all suggest that cycles are present within the unit however all studies utilize different lithofacies in their analysis, making them difficult to compare. Unlike earlier studies that lumped all dolostones as the same lithofacies, more detailed study of the dolostones suggests that there are two lithofacies present (L1 and L2). This observation has significantly revised the interpretation of the cycles. In the model presented here, the structureless dolostones of Lithofacies 1 represent the most offshore, subtidal environment present in the Monkton. Lithofacies 2, the cryptalgalaminite dolostone represents the peri-to supratidal setting.

The most complete cycle identified in the upper Monkton was Lithofacies 6 overlain by Lithofacies 5, Lithofacies 3 and capped by Lithofacies 2. This is a very characteristic shallowing-up cycle, (or parasequence), and it is similar to that described by Rahmanian (1981) for the Monkton. In this cycle, terrigenous subtidal sediments of a sand shoal system are succeeded up section by mixed sediments of the intertidal sand flat and capped by the carbonate sediments of the supratidal. In the analysis by Harding, the architecture is similar: cross bedded sandstones with scoured bases overlain by sand-shale couplets and massive sands and capped by dolostones. They are, however, not as common as condensed sequences, where one or more of these lithofacies are missing. For example, commonly occurring at Salmon Hole (Figure 4) is Lithofacies 1 grading into Lithofacies 5 and then capped by Lithofacies 3. The contact of rippled sands and shales with overlying structureless dolostones represents a flooding event, or in Sequence Stratigraphy terms, a Marine Flooding Surface (MFS). Condensed sequences are represented, for example, by Lithofacies 5 overlain by Lithofacies 3. Cycles average 25 cm in thickness.

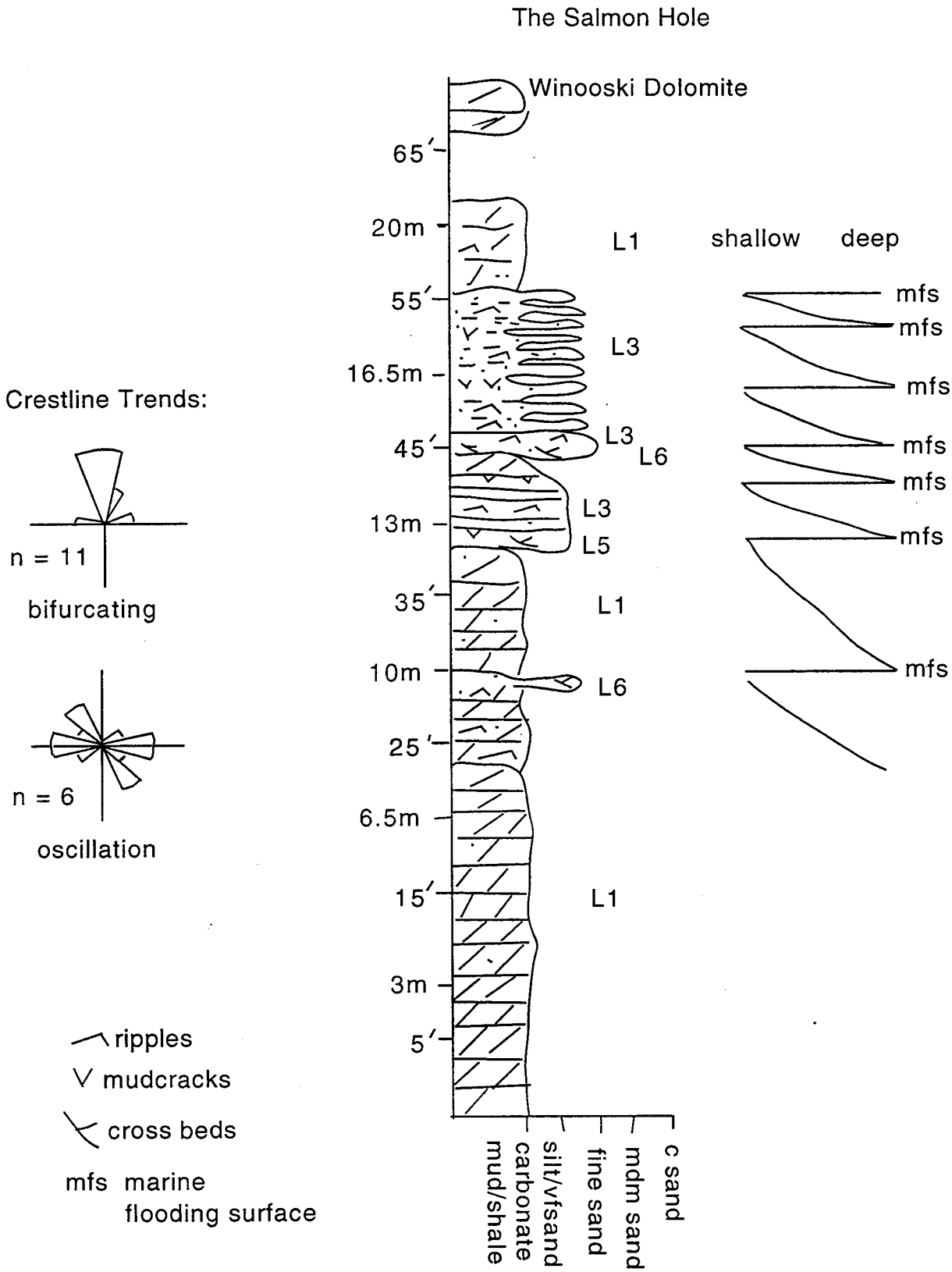

Figure 4. Measured stratigraphic section for Salmon Hole.

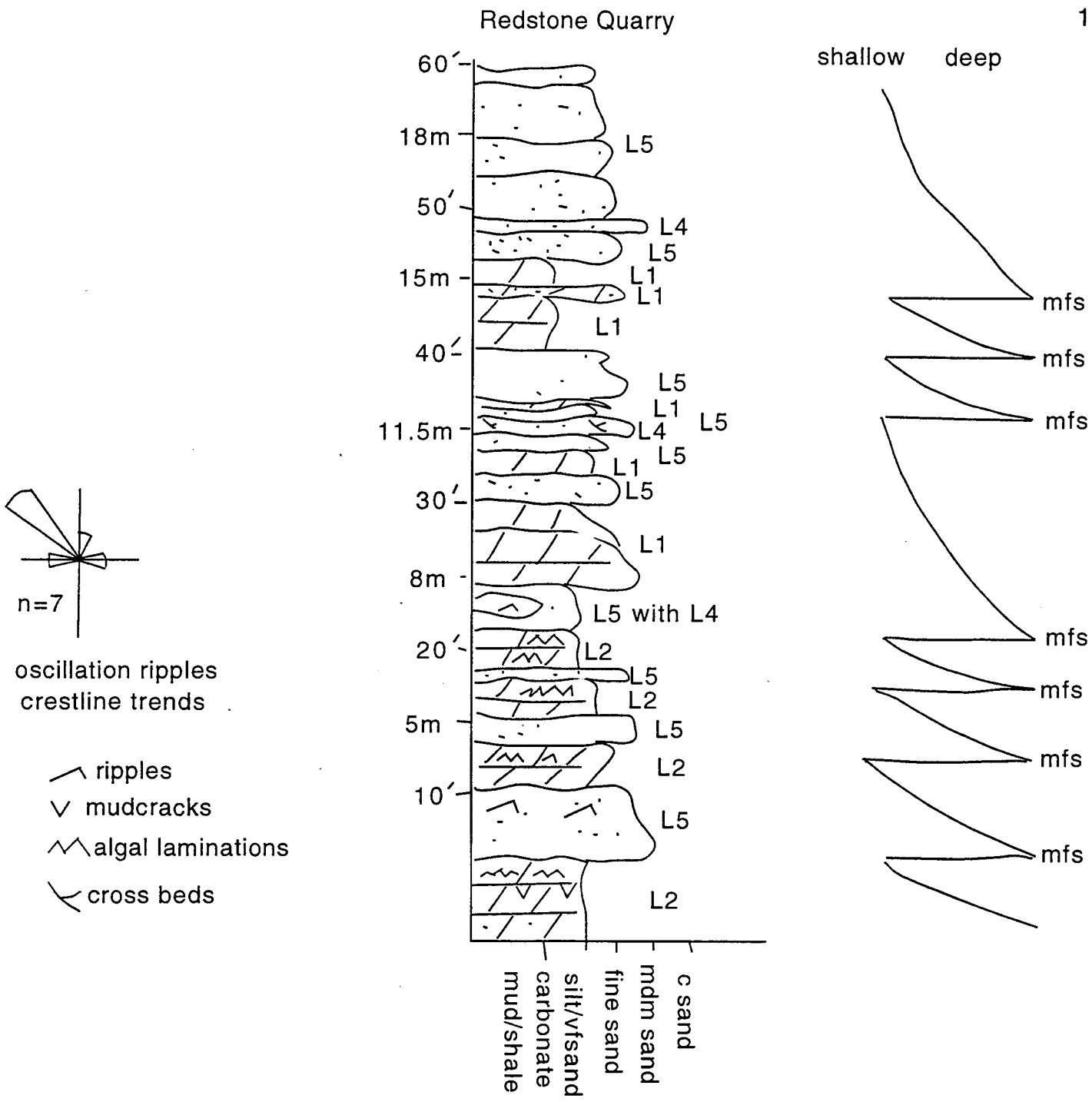

Figure 5. Measured stratigraphic section for Redstone Quarry.

At Redstone Quarry (Figure 5) the architecture is different. Here, cycles consist of Lithofacies 5 or 6 overlain by Lithofacies 3 and capped by Lithofacies 2. Environmentally, this records subtidal sands being overlain by rippled tidal flat sands and shales which grade up into peri-supratidal cryptalgalaminites. The contact of the cryptalgalaminites with overlying sandstones represents the Marine Flooding Surface (MFS). Cycles average 40 cm in thickness.

FIELD TRIP STOPS

Both of these field trip stops are excellent for students in that they expose a wide variety of sedimentary structures and rock types. Over 300 UVM students per year visit both the Salmon Hole and Redstone Quarry localities and the "no hammer" policy is very important for maintaining the quality of the exposures.

Most students, even at the introductory level, come to an environmental interpretation of the Monkton here as a tidally-influenced deposit based on the mudcracks, ripple type and orientation, and alternating grain sizes. Field trips end with interesting discussions regarding sedimentation rates and the time represented by the rocks at these two outcrops. More advanced classes (Strat/Sed) visit these outcrops to do paleocurrent studies and learn detailed section measurement and description. Our sophomore-level Field Geology class learns to measure section and make their first geologic map at the Salmon Hole.

1. Salmon Hole

Location: Riverside Drive, Burlington. Burlington 7.5 minute quad. 0.1 mile from Winooski Bridge. (Figure 6)

Pull into the small parking area off Riverside Drive, where the view looks down on the Salmon Hole. The red-colored Monkton lies below, and the buff-colored Winooski Dolomite to the right, below the bridge and Champlain Mill apartments. Follow the well marked path (flanked by a wall of imported Potsdam Sandstone!) down to the bedding planes on the river. This is a no-hammer outcrop and is part of the Winooski River Valley natural corridor.

When you arrive at the base of the path you are on the uppermost beds of the Monkton. The buff-colored east wall is the overlying Winooski Dolostone. The bedding plane exhibits a variety of excellent oscillation and bifurcating ripples as well as horizontal traces of the *Cruziana* ichnofacies. Carefully descend to the next large bedding plane, passing mudcracked horizons. On the lower bedding plane it is possible to view several meters of Lithofacies 3 in cross section. Note the lateral pinching of the sandstone-shale and dolostone couplets. Due to weathering of the carbonate cement in the sandstone beds the internal laminae of ripples is excellently exposed. One of the laterally discontinuous sandstone beds of Lithofacies 6 - with the suggestion of herringbone cross stratification - is exposed on the northwest corner of the cliff. Depending on the water level in the Winooski River you can continue down section where horizons of structureless dolostone (Lithofacies 1), Lithofacies 5 and Lithofacies 3 occur in several cycles.

Before leaving the large bedding plane and heading back up the path, examine the uppermost bed of Monkton: Lithofacies 1, dolostone with disseminated terrigenous material in planar

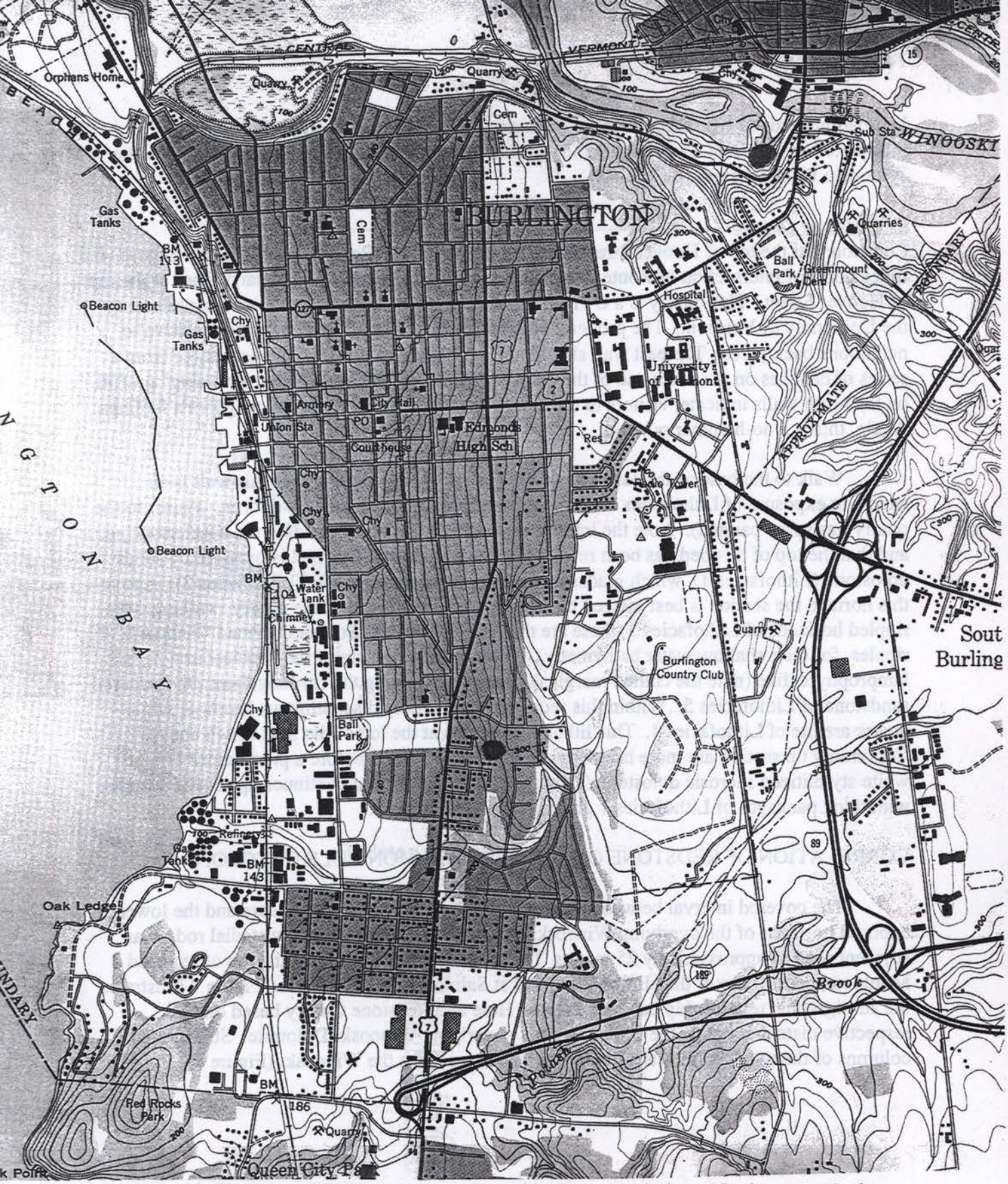

Figure 6. Location of field trip stops indicated by large black dots. Northern stop is the Salmon Hole, southern stop is Redstone Quarry.

laminations and ripples sharply overlies Lithofacies 3 rippled sandstones; this contact is interpreted to represent a marine flooding surface. There is a thin covered interval below the Winooski Dolostone.

2. Redstone Quarry

Location: At the top of Hoover Street, off (east of) Shelburne Road (Route 7) in Burlington. 0.8 miles north of intersection of Route 7 with I-189 (Figure 6). Park on the quarry floor at the top of Hoover Street. This quarry is a UVM Natural Area, an educational resource maintained by the University of Vermont. The property boundaries are not well marked, so be sensitive to neighbor's back yards. The east wall should not be climbed as horizons are accessible from a series of benches on the north end of the quarry. Unfortunately, as the "no trespassing" graffiti on the north walls indicate, visitors to the quarry need to be sensitive to the neighbor's feelings. Again, this is a no-hammer outcrop.

Walk to the base of the east wall of the quarry. At the very base of this wall is an excellent exposure of Lithofacies 6. The cross-bedded sandstone (which a former visitor to the quarry has spray painted). Note the internal structure of this bed, including the basal scouring, and that the top of this bed has been reworked by wave action. This bed is overlain by sandy dolostone (Lithofacies 1), which grades upward into cryptalgalaminite (Lithofacies 2). Above this horizon the section is best viewed by moving to the north end of the quarry, walking over rippled horizons of Lithofacies 3 (these are the ripples that John Southard termed "dishpan" ripples, for their shallow water bathymetry). Walk to the exposure of the Cretaceous lamprophyre dike (note the chilled margins). Sharply overlying the cryptalgalaminite is the red sandstone of Lithofacies 5. Within this sequence are laterally discontinuous layers of white quartz arenite of Lithofacies 4. This lithofacies occurs at the top of the next bench above. Continuing up section are more horizons of Lithofacies 3 and 5 before a pronounced bed of white stylolitized sucrosic dolostone (Lithofacies 1). The section continues up several benches with thick packages of Lithofacies 1 grading into Lithofacies 5.

CORRELATION OF REDSTONE QUARRY AND SALMON HOLE OUTCROPS

The covered interval between the top of the Redstone Quarry exposure and the lowest exposed horizons of the overlying Winooski Dolomite can be measured by stadial rod on an adjacent road as approximately 25 meters. The covered interval between the top of exposed Monkton and the base of the cliff of Winooski at Salmon Hole is 4 meters. Figure 7 illustrates the stratigraphic relationship between Salmon Hole and Redstone Quarry based on their respective distances below the contact with the overlying Winooski Dolomite. Stratigraphic columns of the two localities are "hung" on the contact with the Winooski (Figure 7).

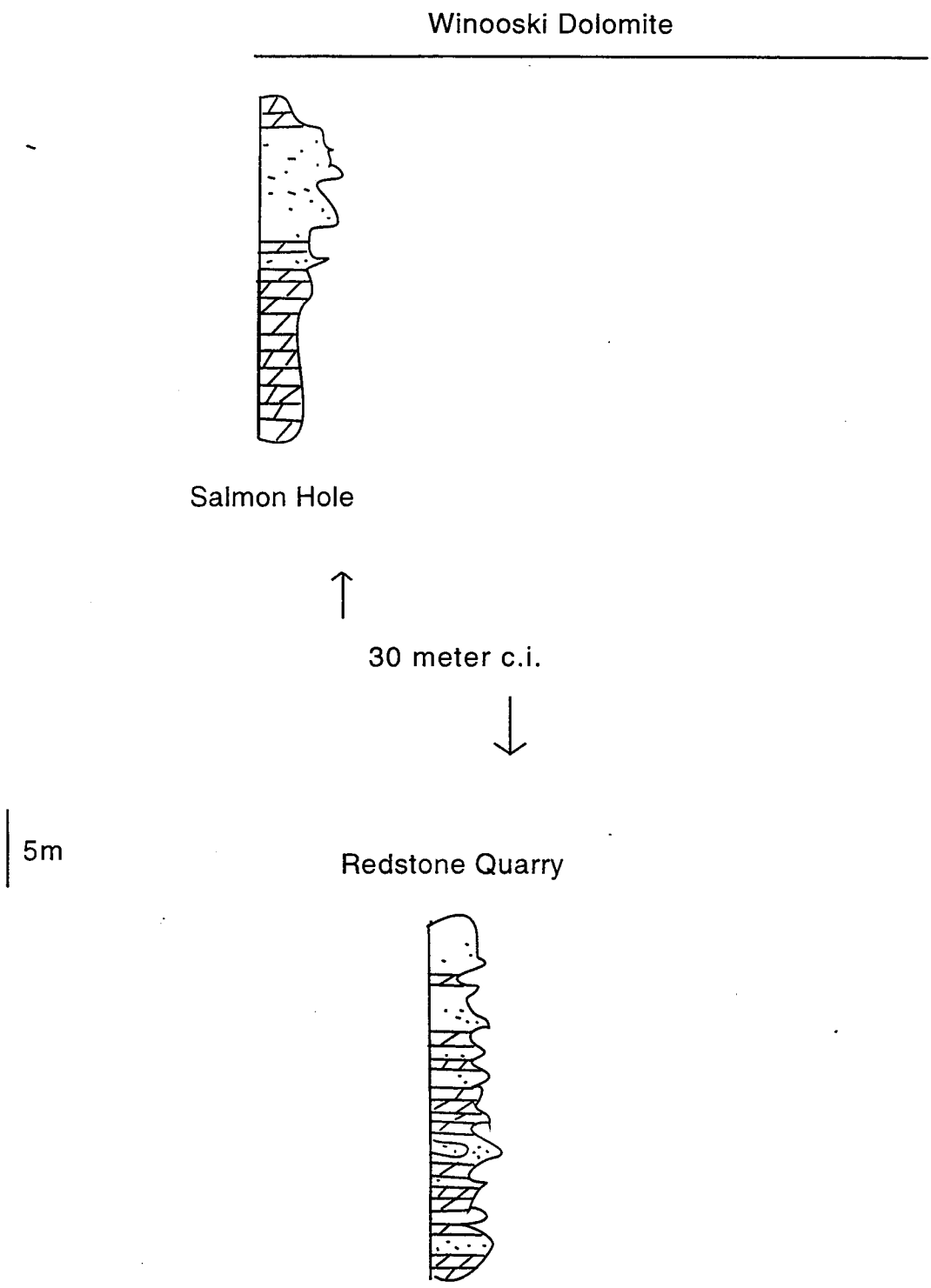

Figure 7. Stratigraphic columns for Salmon Hole and Redstone Quarry hung on the overlying Winooski Dolomite.

REFERENCES CITED

Cady, W., 1945, Stratigraphy and Structure of west-central Vermont: Geol. Soc. of America Bull., v.56, p.515-558.

Dowling, W., 1988, Depositional Environments of the Lower Oak Hill Group, southern Quebec: Implications for the Late Precambrian Breakup of North America in the Quebec Reentrant, unpub. M.S. Thesis, University of Vermon.t

Godin, P.,1991, Fining-upward cycles in the sandy braided-river deposits of the Westwater Canyon Member (Upper Jurassic), Morrison Formation, New Mexico. Sediment. Geol. Vol. 70, p.61-82.

Goldberg, J. and C. Mehrtens, 1998, Depositional Environment and Sequence Stratigraphy interpretation of the Lower Middle Cambrian Monkton Quartzite, Vermont, Northeastern Geology, vol. 20, pp. 11-27.

Gregory, G., 1984, Paleoenvironments of the Dunham Dolomite (Lower Cambrian) of northwestern Vermont, unpub. M.S. Thesis, Univ. Vermont, 180 pp.

James, N., R. Stevens, C. Barnes, I. Knight, 1989, Evolution of a Lower Paleozoic Continental Margin Carbonate Platform, northern Canadian Appalachians, in: P. Crevello, P. Wilson, J.Sarg, J. Read, eds., Controls on Carbonate Platform and Basin Development, Soc. Econ. Paleon. And Mineral., Sp. Pub. 44, pp. 123-146.

Mehrtens, C. and M.A .Borre, 1989, Stratigraphy and Bedrock Geology of Parts of the Colchester and Georgia Plains Quadrangles, Vermont. Vermont Geol. Survey Sp. Bull. No. 10, 35 pp.

Mehrtens, C. and R. Dorsey, 1987, Stratigraphy and Bedrock Geology of a Portion of the St. Albans and Adjacent Highgate Center Quadrangles, Vermont. Vermont Geol.Surv. Sp. Bull. No. 9.

Mehrtens, C. and A. Hadley, 1995, Stratigraphy and Bedrock Geology of a Portion of the St. Albans Quadrangle, Vermont. Vermont Geol. Surv. Sp. Bull. No. 14, 22 pp.

Myrow, P., 1983, Sedimentology of the Cheshire Formation in west-central Vermont, unpub. M.S. Thesis, Univ. Vermont, 177 pp.

Palmer, A., 1971, Cambrian of the Appalachians and eastern New England Regions, eastern U.S.: in, Holland, C., ed. The Cambrian of the New World, p.167-217.

Palmer, A. and N. James, 1979, The Hawke Bay Event: a Circum-Iapetus Event of Lower Cambrian age, In Wones, D.,ed. The Caledonides in the U.S.A.: Blacksburg, Virginia Polytechnic institute and State University memoir 2, p. 15-18.

Posamentier, H. and P. Vail, 1988, Eustatic controls on Clastic Deposition II - Sequence and systems Tract Models: in Wilgus, C., Hastings, B., C. Kendall, H. Posamentier, C. Ross, and J. Van Wagoner, eds., Sea-Level Changes: An Integrated Approach: Soc. Econ. Paleont. and Mineral. Sp. Pub. No 42., p. 125-154.

Rahmanian, V., 1981, Mixed Siliciclastic-Carbonate Tidal Sedimentation in the Lower Cambrian Monkton Formation in west-central Vermont. Geol. Soc. Am. Abstr with Progr., vol. 13, p. 170-171.

Reinecke, H-E. and I.B. Singh, 1975, Depositional Sedimentary Environments, Springer-Verlag, Berlin, 439 pp.

Rogers, J., 1968, The Eastern Edge of the North American Continent During the Cambrian and Early Ordovician: in E-An Zen, W. White, J. Hadley and J. Thompson, eds., Studies in Appalachian Geology, Northern and Maritime, Wiley Interscience, New York, 475 pp.

Shaw, A., 1962, Paleontology of northwestern Vermont IX. Fauna of the Monkton Quartzite. Jour. Paleont., v. 36, p. 322-335.

Vail,P., Mitchum, R. and Thompson, S., 1977, Seismic Stratigraphy and Global Changes in Sea Level, part 4: in Clayton, C., ed. Seismic Stratigraphy - Applications to Hydrocarbon Exploration: Am. Assoc. Petrol Geol. Mem. 26, p. 83-97.

Van Wagoner, J. and G. Bertram, 1993, Sequence Stratigrpahy of Foreland Basin Deposits: Outcrop and Subsurface Examples from the Cretaceous of North America, Am. Assoc. Petrol. Geol. Mem. 64.

Welby, C., 1961, Bedrock geology of the central Champlain Valley: Vermont Development Bull. No. 14, 296 pp.

The Champlain thrust fault, Lone Rock Point, Burlington, Vermont

Rolfe S. Stanley, Department of Geology, University of Vermont, Burlington, Vermont 05405

LOCATION

The 0.6 mi (1 km) exposure of the Champlain thrust fault is located on the eastern shore of Lake Champlain at the north end of Burlington Harbor. The property is owned by the Episcopal Diocesan Center. Drive several miles (km) north along North Avenue (Vermont 127) from the center of Burlington until you reach the traffic light at Institute Road, which leads to Burlington High School, The Episcopal Diocesan Center, and North Beach. Turn west toward the lake and take the first right (north) beyond Burlington High School. The road is marked by a stone archway. Stop at the second building on the west side of the road, which is the Administration Building (low rectangular building), for written permission to visit the field site.

Continue north from the Administration Building, cross the bridge over the old railroad bed, and keep to the left as you drive over a small rise beyond the bridge. Go to the end of this lower road. Park your vehicle so that it does not interfere with the people living at the end of the road (Fig. 1). Walk west from the parking area to the iron fence at the edge of the cliff past the outdoor altar where you will see a fine view of Lake Champlain and the Adirondack Mountains. From here walk south along a footpath for about 600 ft (200 m) until you reach a depression in the cliff that leads to the shore (Fig. 1).

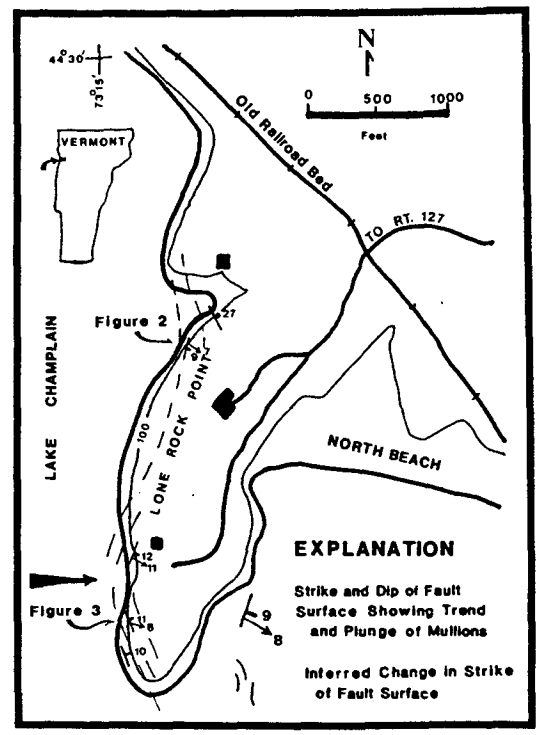

Figure 1. Location map of the Champlain thrust fault at Lone Rock Point, Burlington, Vermont. The buildings belong to the Episcopal Diocesan Center. The road leads to Institute Road and Vermont 127 (North Avenue). The inferred change in orientation of the fault surface is based on measured orientations shown by the dip and strike symbols. The large eastward-directed arrow marks the axis of a broad, late syncline in the fault zone. The location of Figures 2 and 3 are shown to the left of "Lone Rock Point." The large arrow points to the depression referred to in the text.

SIGNIFICANCE

This locality is one of the finest exposures of a thrust fault in the Appalachians because it shows many of the fault zone features characteristic of thrust faults throughout the world. Early studies considered the fault to be an unconformity between the strongly-tilted Ordovician shales of the "Hudson River Group" and the overlying, gently-inclined dolostones and sandstones of the "Red Sandrock Formation" (Dunham, Monkton, and Winooski formations of Cady, 1945), which was thought to be Silurian because it was lithically similar to the Medina Sandstone of New York. Between 1847 and 1861, fossils of pre-Medina age were found in the "Red Sandrock Formation" and its equivalent "Quebec Group" in Canada. Based on this information, Hitchcock and others (1861, p. 340) concluded that the contact was a major fault of regional extent. We now know that it is one of several very important faults that floor major slices of Middle Proterozoic continental crust exposed in western New England.

Our current understanding of the Champlain thrust fault and its associated faults (Champlain thrust zone) is primarily the result of field studies by Keith (1923, 1932), Clark (1934), Cady (1945), Welby (1961), Doll and others (1961), Coney and others (1972), Stanley and Sarkisian (1972), Dorsey and others (1983), and Leonard (1985). Recent seismic reflection studies by Ando and others (1983, 1984) and private industry have shown that the Champlain thrust fault dips eastward beneath the metamorphosed rocks of the Green Mountains. This geometry agrees with earlier interpretations shown in cross sections across central and northern Vermont (Doll and others, 1961; Coney and others, 1972). Leonard's work has shown that the earliest folds and faults in the Ordovician sequence to the west in the Champlain Islands are genetically related to the development of the Champlain thrust fault.

In southern Vermont and eastern New York, Rowley and others (1979), Bosworth (1980), Bosworth and Vollmer (1981), and Bosworth and Rowley (1984), have recognized a zone of late post-cleavage faults (Taconic Frontal Thrust of Bosworth and Rowley, 1984) along the western side of the Taconic Mountains. Rowley (1983), Stanley and Ratcliffe (1983, 1985), and Ratcliffe (in Zen and others, 1983) have correlated this zone with the Champlain thrust fault. If this correlation is correct then the Champlain thrust zone would extend from Rosenberg, Canada, to the Catskill Plateau in east-central New York, a distance of 199 mi (320 km), where it appears to be overlain by Silurian and Devonian rocks. The COCORP line through southern Vermont

shows an east-dipping reflection that roots within Middle Proterozoic rocks of the Green Mountains and intersects the earth's surface along the western side of the Taconic Mountains (Ando and others, 1983, 1984).

The relations described in the foregoing paragraphs suggest that the Champlain thrust fault developed during the later part of the Taconian orogeny of Middle to Late Ordovician age. Subsequent movement, however, during the middle Paleozoic Acadian orogeny and the late Paleozoic Alleghenian orogeny can not be ruled out. The importance of the Champlain thrust in the plate tectonic evolution of western New England has been discussed by Stanley and Ratcliffe (1983, 1985). Earlier discussions can be found in Cady (1969), Rodgers (1970), and Zen (1972).

REGIONAL GEOLOGY

In Vermont the Champlain thrust fault places Lower Cambrian rocks on highly-deformed Middle Ordovician shale. North of Burlington the thrust surface is confined to the lower part of the Dunham Dolomite. At Burlington, the thrust surface cuts upward through 2,275 ft (700 m) of the Dunham into the thick-bedded quartzites and dolostones in the very lower part of the Monkton Quartzite. Throughout its extent, the thrust fault is located within the lowest, thick dolostone of the carbonate-siliciclastic platform sequence that was deposited upon Late Proterozoic rift-clastic rocks and Middle Proterozoic, continental crust of ancient North America.

At Lone Rock Point in Burlington the stratigraphic throw is about 8,850 ft (2,700 m), which represents the thickness of rock cut by the thrust surface. To the north the throw decreases as the thrust surface is lost in the shale terrain north of Rosenberg, Canada. Part, if not all, of this displacement is taken up by the Highgate Springs and Philipsburg thrust faults that continue northward and become the "Logan's Line" thrust of Cady (1969). South of Burlington the stratigraphic throw is in the order of 6,000 ft (1,800 m). As the throw decreases on the Champlain thrust fault in central Vermont the displacement is again taken up by movement on the Orwell, Shoreham, and Pinnacle thrust faults.

Younger open folds and arches that deform the Champlain slice may be due either duplexes or ramps along or beneath the Champlain thrust fault. To the west, numerous thrust faults are exposed in the Ordovician section along the shores of Lake Champlain (Hawley, 1957; Fisher, 1968; Leonard, 1985). One of these broad folds is exposed along the north part of Lone Rock Point (Fig. 2). Based on seismic reflection studies in Vermont, duplex formation as described by Suppe (1982) and Boyer and Elliot (1982) indeed appears to be the mechanism by which major folds have developed in the Champlain slice.

North of Burlington the trace of the Champlain thrust fault is relatively straight and the surface strikes north and dips at about 15° to the east. South of Burlington the trace is irregular because the thrust has been more deformed by high-angle faults and broad folds. Slivers of dolostone (Lower Cambrian Dunham Dolomite) and limestone (Lower Ordovician Beekmantown Group) can be found all along the trace of the thrust. The limestone represents

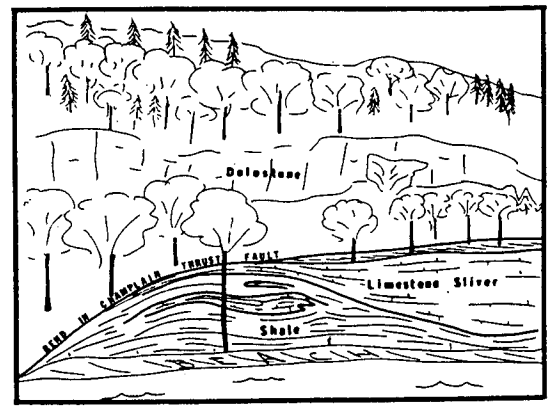

Figure 2. A sketch of the Champlain thrust fault at the north end of Lone Rock Point showing the large bend in the fault zone and the slivers of Lower Ordovician limestone. The layering in the shale is the S1 cleavage. It is folded by small folds and cut by many generations of calcite veins and faults. The sketch is located in Figure 1.

fragments from the Highgate Springs slice exposed directly west and beneath the Champlain thrust fault north of Burlington (Doll and others, 1961). In a 3.3 to 10 ft (1 to 3 m) zone along the thrust surface, fractured clasts of these slivers are found in a matrix of ground and rewelded shale.

Estimates of displacement along the Champlain thrust fault have increased substantially as a result of regional considerations (Palmer, 1969; Zen and others, 1983; Stanley and Ratcliffe, 1983, 1985) and seismic reflection studies (Ando and others, 1983, 1984). The earlier estimates were less than 9 mi (15 km) and were either based on cross sections accompanying the Geologic Map of Vermont (Doll and others, 1961) or simply trigonometric calculations using the average dip of the fault and its stratigraphic throw. Current estimates are in the order of 35 to 50 mi (60 to 80 km). Using plate tectonic considerations, Rowley (1982) has suggested an even higher value of 62 mi (100 km). These larger estimates are more realistic than earlier ones considering the regional extent of the Champlain thrust fault.

Lone Rock Point

At Lone Rock Point the basal part of the Lower Cambrian Dunham Dolostone overlies the Middle Ordovician Iberville Formation. Because the upper plate dolostone is more resistent than the lower plate shale, the fault zone is well exposed from the northern part of Burlington Bay northward for approximately 0.9 mi (1.5 km; Fig. 1). The features are typical of the Champlain thrust fault where it has been observed elsewhere.

The Champlain fault zone can be divided into an inner and outer part. The inner zone is 1.6 to 20 ft (0.5 to 6 m) thick and consists of dolostone and limestone breccia encased in welded, but highly contorted shale (Fig. 3). Calcite veins are abundant. One of the most prominent and important features of the inner fault zone is the slip surface, which is very planar and continuous throughout the exposed fault zone (Fig. 3). This surface is marked by very fine-grained gouge and, in some places, calcite slickenlines. Where the inner fault zone is thin, the slip surface is located

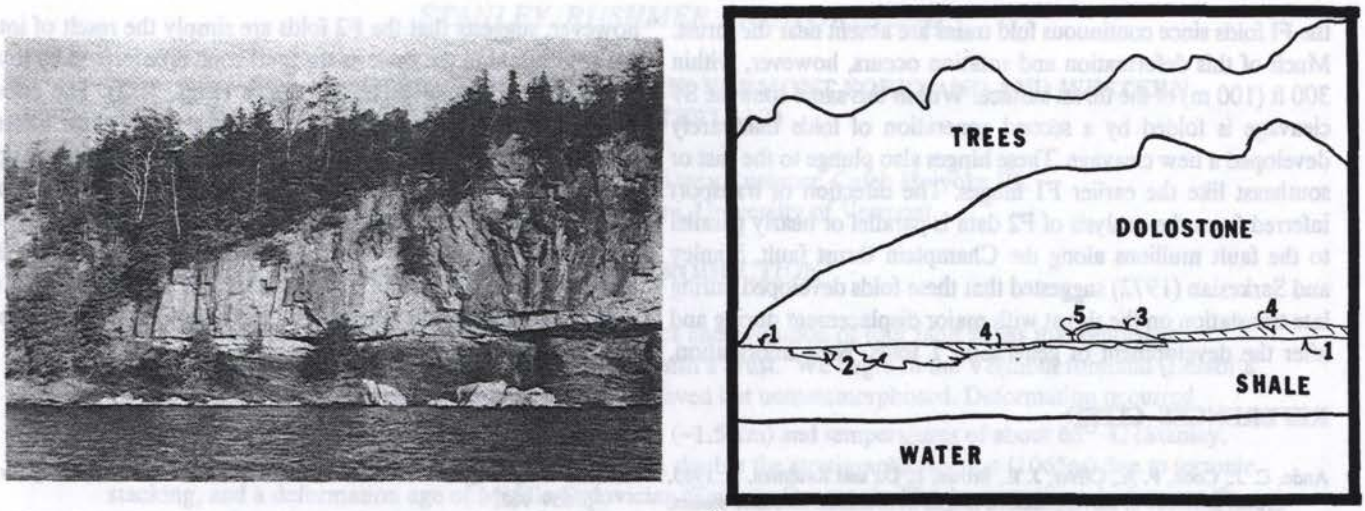

Figure 3. View of the Champlain thrust fault looking east at the southern end of Lone Rock Point (Fig. 1). The accompanying line drawing locates by number the important features discussed in the text: 1, the continuous planar slip surface; 2, limestone slivers; 3, A hollow in the base of the dolostone is filled in with limestone and dolostone breccia; 4, Fault mullions decorate the slip surface at the base of the dolostone; 5, a small dike of shale has been injected between the breccia and the dolostone.

along the interface between the Dunham Dolomite and the Iberville Shale. Where the inner fault is wider by virtue of slivers and irregularities along the basal surface of the Dunham Dolomite, the slip surface is located in the shale, where it forms the chord between these irregularities (Fig. 3). The slip surface represents the surface along which most of the recent motion in the fault zone has occurred. As a consequence, it cuts across all the irregularities in the harder dolostone of the upper plate with the exception of long wave-length corrugations (fault mullions) that parallel the transport direction. As a result, irregular hollows along the base of the Dunham Dolomite are filled in by highly contorted shales and welded breccia (Fig. 3).

The deformation in the shale beneath the fault provides a basis for interpreting the movement and evolution along the Champlain thrust fault. The compositional layering in the shale of the lower plate represents the well-developed S1 pressure-solution cleavage that is essentially parallel to the axial planes of the first-generation of folds in the Ordovician shale exposed below and to the west of the Champlain thrust fault (Fig. 4). As the trace of the thrust fault is approached from the west this cleavage is rotated eastward to shallow dips as a result of westward movement of the upper plate (Fig. 4). Slickenlines, grooves, and prominent fault mullions on the lower surface of the dolostone and in the adjacent shales, where they are not badly deformed by younger events, indicate displacement was along an azimuth of approximately N60°W (Fig. 4; Hawley, 1957; Stanley and Sarkesian, 1972; Leonard, 1985). The S1 cleavage at Lone Rock Point is so well developed in the fault zone that folds in the original bedding are largely destroyed. In a few places, however, isolated hinges are preserved and are seen to plunge eastward or southeastward at low angles (Fig. 4). As these F1 folds are traced westward from the fault zone, their hinges change orientation to the northeast. A similar geometric pattern is seen along smaller faults, which deform S1 cleavage in the Ordovician rocks west of the Champlain thrust fault. These relations suggest that F1 hinges are rotated towards the transport direction as the Champlain thrust fault is approached. The process involved fragmentation of

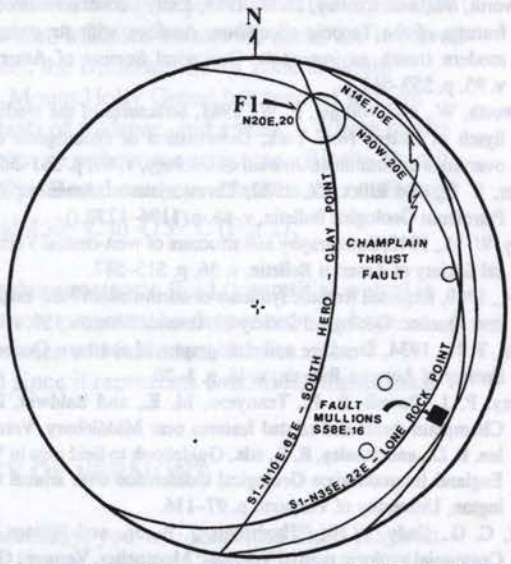

Figure 4. Lower hemisphere equal-area net showing structural elements associated with the Champlain thrust fault. The change in orientation of the thrust surface varies from approximately N20°W to N14°E at Lone Rock Point. The orientation of S1 cleavage directly below the thrust is the average of 40 measurements collected along the length of the exposure. S1, however, dips steeply eastward in the Ordovician rocks to the west of the Champlain thrust fault as seen at South Hero and Clay Point where F1 hinges plunge gently to the northeast. Near the Champlain thrust fault F1 hinges (small circles) plunge to the east. Most slickenlines in the adjacent shale are approximately parallel to the fault mullions shown in the figure.

the FI folds since continuous fold trains are absent near the thrust. Much of this deformation and rotation occurs, however, within 300 ft (100 m) of the thrust surface. Within this same zone the S1 cleavage is folded by a second generation of folds that rarely developed a new cleavage. These hinges also plunge to the east or southeast like the earlier F1 hinges. The direction of transport inferred from the analysis of F2 data is parallel or nearly parallel to the fault mullions along the Champlain thrust fault. Stanley and Sarkesian (1972) suggested that these folds developed during late translation on the thrust with major displacement during and after the development of generation 1 folds. New information, however, suggests that the F2 folds are simply the result of internal adjustment in the shale as the fault zone is deformed by lower duplexes and frontal or lateral ramps (Figs. 1, 2). The critical evidence for this new interpretation is the sense of shear inferred from F2 folds and their relation to the broad undulations mapped in the fault zone as it is traced northward along Lone Rock Point (Fig. 1). South of the position of the thick arrow in Figure 1, the inferred shear is west-over-east whereas north of the arrow it is east-over-west. The shear direction therefore changes across the axis of the undulation (marked by the arrow) as it should for a synclinal fold.

REFERENCES CITED

Ando, C. J., Cook, F. A., Oliver, J. E., Brown, L. D., and Kaufman, S., 1983, Crustal geometry of the Appalachian orogen from seismic reflection studies, *in* Hatcher, R. D., Jr., Williams, H., and Zietz, I., eds., Contributions to the tectonics and geophysics of mountain chains: Geological Society of America Memoir 158, p. 83–101.

Ando, C. J., Czuchra, B. L., Klemperer, S. L., Brown, L. D., Cheadle, M. J., Cook, F. A., Oliver, J. E., Kaufman, S., Walsh, T., Thompson, J. B., Jr., Lyons, J. B., and Rosenfeld, J. L., 1984, Crustal profile of mountain belt; COCORP Deep Seismic reflection profiling in New England Appalachians and implications for architecture of convergent mountain chains: American Association of Petroleum Geologists Bulletin, v. 68, p. 819–837.

Bosworth, W., 1980, Structural geology of the Fort Miller, Schuylerville and portions of the Schagticoke 7½-minute Quadrangles, eastern New York and its implications in Taconic geology [Ph.D. thesis]: Part 1, State University of New York at Albany, 237 p.

Bosworth, W., and Rowley, D. B., 1984, Early obduction-related deformation features of the Taconic allochthon; Analogy with structures observed in modern trench environments: Geological Society of American Bulletin, v. 95, p. 559–567.

Bosworth, W., and Vollmer, F. W., 1981, Structures of the medial Ordovician flysch of eastern New York; Deformation of synorogenic deposits in an overthrust environment: Journal of Geology, v. 89, p. 551–568.

Boyer, S. E., and Elliot, D., 1982, Thrust systems: American Association of Petroleum Geologists Bulletin, v. 66, p. 1196–1230.

Cady, W. M., 1945, Stratigraphy and structure of west-central Vermont: Geological Society of America Bulletin, v. 56, p. 515–587.

—— , 1969, Regional tectonic synthesis of northwestern New England and adjacent Quebec: Geological Society of America Memoir 120, 181 p.

Clark, T. H., 1934, Structure and stratigraphy of southern Quebec: Geological Society of America Bulletin, v. 45, p. 1–20.

Coney, P. J., Powell, R. E., Tennyson, M. E., and Baldwin, B., 1972, The Champlain thrust and related features near Middlebury, Vermont, *in* Doolan, B. D., and Stanley, R. S., eds., Guidebook to field trips in Vermont, New England Intercollegiate Geological Conference 64th annual meeting: Burlington, University of Vermont, p. 97–116.

Doll, C. G., Cady, W. M., Thompson, J. B., Jr., and Billings, M. P., 1961, Centennial geologic map of Vermont: Montpelier, Vermont Geological Survey, scale 1:250,000.

Dorsey, R. L., Agnew, P. C., Carter, C. M., Rosencrantz, E. J., and Stanley, R. S., 1983, Bedrock geology of the Milton Quadrangle, northwestern Vermont: Vermont Geological Survey Special Bulletin No. 3, 14 p.

Fisher, D. W., 1968, Geology of the Plattsburgh and Rouses Point Quadrangles, New York and Vermont: Vermont Geological Survey Special Publications No. 1, 51 p.

Hawley, D., 1957, Ordovician shales and submarine slide breccias of northern Champlain Valley in Vermont: Geological Society of America Bulletin, v. 68, p. 155–194.

Hitchcock, E., Hitchcock, E., Jr., Hager, A. D., and Hitchcock, C., 1861, Report on the geology of Vermont: Clairmont, Vermont, v. 1, 558 p.; v. 2, p. 559–988.

Keith, A., 1923, Outline of Appalachian structures: Geological Society of America Bulletin, v. 34, p. 309–380.

—— , 1932, Stratigraphy and structure of northwestern Vermont: American Journal of Science, v. 22, p. 357–379, 393–406.

Leonard, K. E., 1985, Foreland fold and thrust belt deformation chronology, Ordovician limestone and shale, northwestern Vermont [M.S. thesis]: Burlington, University of Vermont, 138 p.

Palmer, A. R., 1969, Stratigraphic evidence for magnitude of movement on the Champlain thrust: Geological Society of America, Abstract with Programs, Part 1, p. 47–48.

Rodgers, J., 1970, The tectonics of the Appalachians: New York, Wiley Interscience, 271 p.

Rowley, D. B., 1982, New methods for estimating displacements of thrust faults affecting Atlantic-type shelf sequences; With applications to the Champlain thrust, Vermont: Tectonics, v. 1, no. 4, p. 369–388.

—— , 1983, Contrasting fold-thrust relationships along northern and western edges of the Taconic allochthons; Implications for a two-stage emplacement history: Geological Society of America Abstracts with Programs, v. 15, p. 174.

Rowley, D. B., Kidd, W.S.F., and Delano, L. L., 1979, Detailed stratigraphic and structural features of the Giddings Brook slice of the Taconic Allochthon in the Granville area, *in* Friedman, G. M., ed., Guidebook to field trips for the New York State Geological Association and the New England Intercollegiate Geological Conference, 71st annual meeting: Troy, New York, Rensselaer Polytechnical Institute, 186–242.

Stanley, R. S., and Ratcliffe, N. M., 1983, Simplified lithotectonic synthesis of the pre-Silurian eugeoclinal rocks of western New England: Vermont Geological Survey Special Bulletin No. 5.

—— , 1985, Tectonic synthesis of the Taconic orogeny in western New England: Geological Society of America Bulletin, v. 96, p. 1227–1250.

Stanley, R. S., and Sarkesian, A., 1972, Analysis and chronology of structures along the Champlain thrust west of the Hinesburg synclinorium, *in* Doolan, D. L., and Stanley, R. S., eds., Guidebook for field trips in Vermont, 64th annual meeting of the New England Intercollegiate Geological Conference, Burlington, Vermont, p. 117–149.

Suppe, J., 1982, Geometry and kinematics of fault-related parallel folding: American Journal of Science, v. 282, p. 684–721.

Welby, C. W., 1961, Bedrock geology of the Champlain Valley of Vermont: Vermont Geological Survey Bulletin No. 14, 296 p.

Zen, E-an, 1972, The Taconide zone and the Taconic orogeny in the western part of the northern Appalachian orogen: Geological Society of America Special Paper 135, 72 p.

Zen, E-an, ed., Goldsmith, R., Ratcliffe, N. M., Robinson, P., and Stanley, R. S., compilers, 1983, Bedrock geologic map of Massachusetts: U.S. Geological Survey; the Commonwealth of Massachusetts, Department of Public Works; and Sinnot, J. A., State Geologist, scale 1:250,000.

Trip A6: FAULTS AND FLUIDS, THE VERMONT FORELAND AND WESTERN HINTERLAND

Leaders: Rolfe Stanley, Tracy Rushmer, Caleb Holyoke III,
and Andrea Lini, University of Vermont

INTRODUCTION

The focus of this trip will be on the characteristics and evolution of four fault zones that represent behavior at three progressively deeper levels in the earth's crust. We begin in the Vermont foreland (Lessor's Quarry and the Beam, Fig. 1) where the rocks are cleaved but unmetamorphosed. Deformation occurred under confining pressures in the order of 0.5 kilobars (~1.5 km) and temperatures of about 65^0 C (Stanley, 1990, p.238) assuming a normal geothermal gradient, double the stratigraphic section (1065m) due to tectonic stacking, and a deformation age of Middle Ordovician (Taconic Orogeny). Fluid composition is dominantly calcite-bearing, interstitial water, although dehydration of clays can not be totally ruled out in the pressure solution development of the cleavage. After studying this outcrop, we will then travel eastward to the Hinesburg thrust fault where Late Proterozoic to Lower Cambrian rocks of the Fairfield Pond Phyllite and lower part of the Cheshire Quartzite (rift-drift transition) were displaced westward over the Lower Ordovician Bascom Formation (carbonate-siliciclastic platform) (Fig 1). Based on ductile deformation fabrics in quartz, brittle deformation fabrics in feldspar, chlorite-sericite assemblages, and dolomite-quartz veins, confining pressures and temperatures are estimated to be a minimum of 3.5 Kbars (~11 km) and 375^0 C (Fig.2). Fluids in the argillaceous quartzite of the upper plate were saturated in silica as evidenced by numerous generations of quartz veins. These veins record a rich history of deformation. The fluids were enriched in sulphides in the ultramylonites of the fault surface. Quartz-dolomite veins are found in the carbonate slivers of the lower plate. Understanding the origin of the fluids and the history of the veins is critically important in understanding the evolution of the fault zone. We will give you our best interpretation! Our last stops will be along the boundary of the Lincoln massif where Middle Proterozoic rocks are involved with major, biotite-grade, ductile thrust zones (Cobb Hill thrust and the Underhill thrust zone at South Lincoln, Fig 1, Fig.3). Here biotite-quartz-feldspar gneiss of the Mount Holly Group has reacted to form muscovite-quartz mylonites with varying amounts of flattened clasts of feldspar, and gneiss. Where quartz lenses, pods, and veins are present, the mylonites are rich in muscovite or become schistose. Biotite-chlorite schist occurs in the fault zone near amphibolite of the Mount Holly. Based on these relations the confining pressure and temperatures are estimated to be 5 kbars (17 km) and 450^0 C to 475^0 C (Fig.2).

Clearly, the traverse has gone from near-surface conditions where meteoric fluid (interstitial water) is important in pressure solution and brittle deformation (abnormal pore pressure) to deeper zones where metamorphic reactions play a critical role in strain softening processes and fault-zone fabrics. The Hinesburg thrust fault is, in many respects, the most complicated since it represents conditions transitional between the other two.

FLUIDS AND THE GEOLOGY OF VERMONT

After spending some time in the field in Vermont, as you will today, you will sense that fluid plays an active role in many of the features observed in the rock; everything from veining to development of hydrous metamorphic assemblages. Fluid flow has been a "hot" topic in Vermont geology for sometime and has attracted attention world wide as an area in which pervasive, instead of channelized, fluid flow is the rule rather than the exception. This has mainly been studied from a metamorphic point of view. Fluid interaction during deformation, however, has also been documented as these outcrops show beautifully. At these different crustal levels, fluids have clearly been present during deformation. This is significant in that the presence of fluid can create abnormal pore pressures which enables brittle deformation even under pressure and temperature conditions where deformation is macroscopically ductile. In addition, dehydration of sediments can produce mica phases which can localize ductile deformation.

Stanley, R., Rushmer, T., Holyoke, C., and Lini, A., 1999,Faults and fluids in the Vermont foreland and hinterland in western Vermont; in Wright, S.F. ed., New England Intercollegiate Geologic Conference Guidebook Number 91, p. 135–158.

At the "beam" outcrop, the shallowest of our outcrops today and where fluid is trapped interstitially, abnormal pore pressures generated during cleavage development focuses deformation along fluid-lined fractures. As we go deeper into the crust, dehydration of hydrous phases begins to play a role. The origin of the silica-saturated fluid at the Hinesburg Thrust may be derived from the phyllite layers. Quartz veins are evidence of brittle behavior induced when pore pressure increased and stress exceeded what could be accommodated by the ductile deformation mechanisms (mainly accommodated by mylonization focused in the muscovite-rich phyllite layers). Interestingly, this shift to brittle behavior occurred more than once suggesting a cyclic process of fluid build-up and release by fracturing during the development of the fault zone. Finally at the deepest fault zone we see evidence of muscovite growth and free silica produced from a potassium feldspar reaction with water. The water source is likely derived from the dehydration of sediments during burial. The muscovite-rich assemblage is then weaker than surrounding feldspar-rich rocks and can accommodate strain during subsequent deformation.

GEOLOGIC SETTING

Central Vermont provides an excellent field laboratory for studying the tectonic transition between the foreland and the pre-Silurian hinterland of western New England because many of the major lithotectonic units are exposed in a 40 km wide belt (Fig. 1) and the underlying Middle Proterozoic granitic basement of the Green Mountains is present in the Lincoln massif (Fig. 3)

The rocks of the foreland consist of a basal rift-clastic sequence overlain by carbonate and siliciclastic rocks of the platform whereas the rocks of the hinterland consist of metamorphosed pelitic, psammitic, and mafic volcanic rocks of the slope-rise and outer rise sequence (Fig. 1 and Fig. 3). Major west-directed thrust faults (Champlain, Hinesburg, Cobb Hill, Underhill at South Lincoln, for example) cut the section and become more numerous to the east in the hinterland. Some of these faults have brought Middle Proterozoic rocks to the surface (Cobb Hill, Underhill at South Lincoln) whereas others like the Champlain thrust fault can be traced by seismic studies into the Middle Proterozoic basement beneath the Green Mountains. The metamorphic grade ranges from essentially unmetamorphosed, although well lithified and cleaved, sedimentary platform rocks of the foreland to kyanite-chloritoid grade in the hinterland along the Green

---

FIGURE 1 (opposite page) Interpretative Geologic Map of Vermont and eastern New York modified from Stanley and Ratcliffe (1985, pl. 1, Fig. 2A). The following symbols are generally listed from west to east. Yad, Middle Proterozoic of the Adirondack massif; Yg, Middle Proterozoic of the Green Mountain massif; YL, Middle Proterozoic of the Lincoln massif; Y, Middle Proterozoic between the Green Mountain massif (Yg), and the Taconic allochthons (medium grey); OCp, Cambrian and Ordovician rocks of the carbonate-siliciclastic platform (DRIFT STAGE); rift-clastic sequence of the Pinnacle (CZp) and Fairfield Pond Formations (CZf) and their equivalents on the east side of the Lincoln and Green Mountain massifs. CZu, Underhill Formation; CZuj, Jay Peak Member of the Underhill Formation (RIFT STAGE IN HINTERLAND); OCr, include RIFT STAGE rocks of the Pinney Hollow and Stowe Formations; FOREARC SEQUENCE (Missisquoi Group) include Om, Moretown Formation and Oh includes Harlow Bridge and Cram Hill Formations in Vermont and Hawley Formation in Massachusetts. Silurian-Devonian sequence include Shaw Mountain, Northfield and Waits River Formations in the area labelled "Silurian-Devonian Formations". Symbol T in A6 is the glaucophane locality at Tilliston Peak. Short line with X's (Worcester Mountains and Mt Elmore) and line with rhombs (Mount Grant) in C6 and D5 mark the Ordovician kyanite-chloritoid zones of Albee (1968). Widely-spaced diagonal lines in north central Vermont outline the region that contains medium-high pressure amphiboles described by Laird and Albee (1981). Irregular black marks are ultramafic bodies (U). LQ & BEAM UT, Lessor's Quarry and the "Beam", PhT, Philipsburg thrust; HSpt, Highgate Springs thrust; PT, Pinnacle thrust; OT, Orwell thrust; HT, Hinesburg thrust; HTFM, the Hinesburg thrust fault at Mechanicsville; COBB HILL, Cobb Hill thrust fault at Lincoln; UT, Underhill thrust; UTSL, Underhill thrust fault at South Lincoln; JS, Jerusalem slice; US, Underhill slice; HNS, Hazens North slice; MVFZ, Missisquoi Valley fault zone; PHS, Pinney Hollow slice; BMT, Belvidere Mountain thrust; CHT, Coburn Hill thrust; Qa, Ascot-Weedon sequence (?) in grid location 7A.

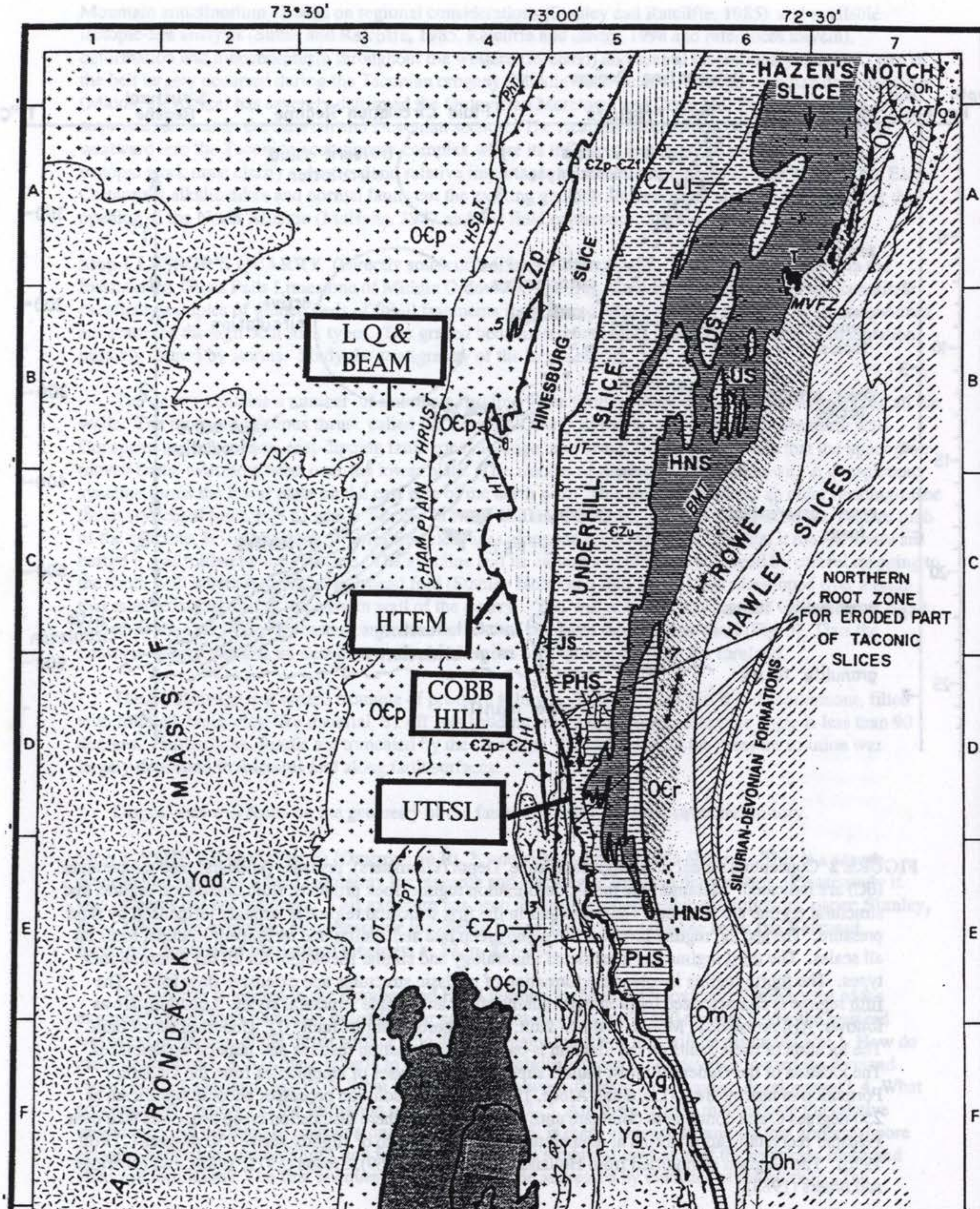
73°30'
73°00'
72°30'
45°00'
44°30'
44°00'
43°30'
HAZEN'S NOTCH SLICE
L Q & BEAM
HTFM
COBB HILL
UTFSL
HINESBURG SLICE
UNDERHILL SLICE
ROWE - HAWLEY SLICES
NORTHERN ROOT ZONE FOR ERODED PART OF TACONIC SLICES
SILURIAN-DEVONIAN FORMATIONS
CHAMPLAIN THRUST
ADIRONDACK MASSIF
HNS
PHS
JS
US
OCp
OCr
CZp
CZuj
Yad
Yg
Om
Oh
MVFZ
BMT
HSpT
HT
UT
CHT
PT
OT

FIGURE 1

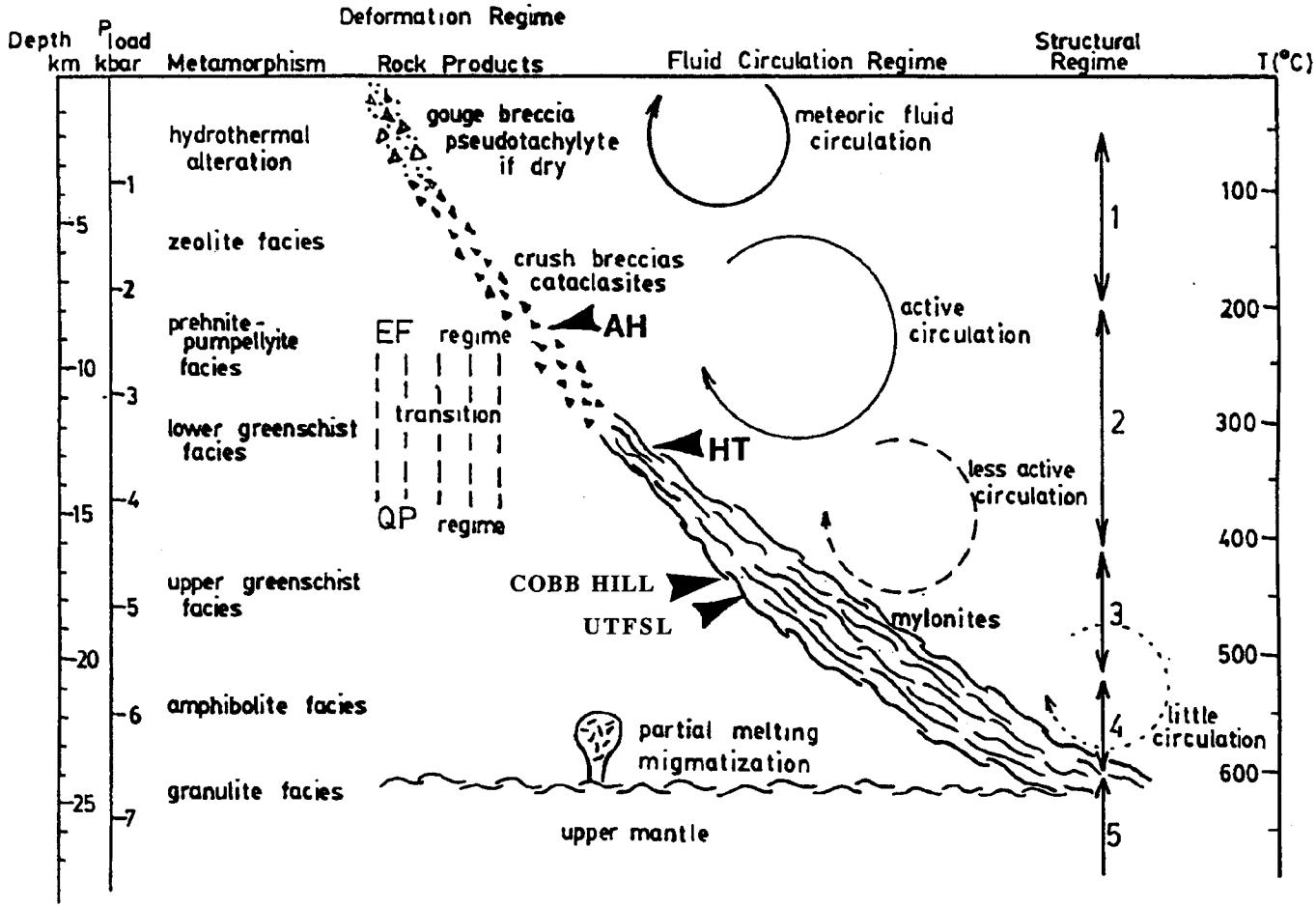

FIGURE 2 Conceptual model of a major fault zone. Depth (kilometers), pressure (kilobars), and temperature (0C) are indicated. Metamorphic facies, deformation regime, rock products, fluid circulation regime, and structural regime are labelled. The behaviour in the first structural regime is strongly influenced by fluid pressure. The second regime involves increased creep rate and similar and recumbent isoclinal folds on all scales. The third regime has a restricted mineralogy and similar rheologies for all the common rock types. The fourth regime involves the formation of gneissic structures and extensive flow folds. The fifth regime is characterized by prolonged laminar flow and simple structural styles. Locations are as follows: AH, Arrowhead Mountain thrust fault; HT, Hinesburg thrust fault; UT, Underhill thrust fault. The location of these faults on the diagram is based on deformation features and mineral assemblages. The location of the Underhill thrust fault is supported by analyses of amphiboles from the Underhill Formation in nearby areas (Laird and Albee, 1981). Pressure solution processes become significant at 250 degrees C and continue to dominate until 400 degrees C where dislocation creep processes take over. Feldspar recrystallization occurs at temperatures that are equal to or slightly above 450 degrees C (Voll, 1976). The diagram is modified from Holland and Lambert (1969), Sibson (1977, 1983), and Etheridge and others (1983).

Mountain anticlinorium. Based on regional considerations (Stanley and Ratcliffe, 1985) and available isotopic-age analysis (Sutter and Ratcliffe, 1985, Ratcliffe and others, 1998 and references therein), deformation and metamorphism throughout the western (foreland) and central (accretionary complex) part of the belt largely occurred during the Taconian orogeny (Middle Ordovician). Younger Acadian deformation (Middle Devonian) has severely deformed the Ordovician Moretown and Cram Hill Formations (fore-arc sequence) as well as the Silurian and Devonian section. The Acadian deformation decreases in intensity westward into the Taconian accretionary complex where its influence is thought to be minimal. Future isotopic work must clarify the extent and relative importance of these two orogenic events. During the Early Cretaceous alkalic dikes and normal faults cut the existing geology and represent abortive rifting during the opening of the North Atlantic (McHone, 1987 and this field conference; Stanley, 1980).

Stop 1 LESSOR'S QUARRY (Directly south off of Sunset View Road) - This quarry is located in the fossiliferous Glens Falls Limestone of Middle Ordovician age (Fig.4 and Fig.5). The Glens Falls contains excellent examples of graded beds of fossil fragments interlayered with laminated micrite. Bryozoan mounds are scattered through both rock types. The graded beds represent distinct pulses of carbonate sedimentation possibly caused by storms. Study the stratigraphy of the larger blocks.

The quarry contains a number of imbricate bedding plane thrusts which can be studied by mapping all the walls. The most conspicuous thrust, called the Lessor's Quarry thrust, is well exposed on the north wall. Conspicuous slickenlines, east-dipping fault-zone cleavage, and bent S1 cleavage indicate that the upper plate moved to the west-northwest over the lower plate. The amount of displacement is unknown. A conspicuous syncline forms the lower plate on the east side of the north wall. This syncline deforms an older bedding-plane thrust (synclinal fault, Fig. 5) which dies out in small faults and pressure solution features on the western limb of the syncline. It is a blind thrust. Multiple cleavages along the blind thrust indicate that it moved westward before it was folded by the syncline. The syncline and its eastern anticline can be traced by careful mapping to the south wall where it forms a fault-bend fold (Stanley fault-bend fold, Fig. 5) that developed over a ramp that must exist just east of the eastern wall of the quarry . You will note that the Lessor's Quarry thrust is not folded by the syncline or its eastern anticline, but instead truncates the synclinal fault (Fig. 5). Thus the Lessor's Quarry thrust is an excellent example of an out-of-sequence thrust in the foreland.

The S1 cleavage is a superb example of pressure solution. You will note that it is discontinuous, filled with foliated, black clay-like material. S1 off sets bedding where the bedding-cleavage angle is less than 90 degrees. Furthermore, fossils are truncated by the cleavage. The calcite from the pressure solution was largely deposited in fractures and along fault surfaces.

Discussions will focus on the geometry of the faults and folds and their structural history.

Stop 2 "THE BEAM" (Fig. 6) (Outcrops on Rt. 2, one mile east of Lessor's Quarry). This is a superb outcrop that serves as a field laboratory for research and teaching of foreland deformation. Please study it. Use cameras but not hammers. This exposure has been thoroughly discussed in the following paper: **Stanley, R.S., 1990, The evolution of mesoscopic imbricate thrust faults - an example from the Vermont foreland: Journal of Structural Geology, v. 12, p. 227-242.**

The outcrop is located in the Cumberland Head Formation (Middle Ordovician) 5 miles west of the exposed front of the Champlain thrust fault or approximately 4600 feet (1400 meters) below the restored westward projection of the thrust surface (Fig.4). The major questions that will be discussed are: 1. How do ramp faults form?, 2. Are there criteria to determine if imbricate thrust faults develop toward the foreland (west) or the hinterland (east)?, 3. What is the relation between faulting and cleavage development?, 4. What processes are involved in the formation of the fault zones?, 5. Are there criteria that indicate the relative importance and duration of motion along the fault zone?, 6. Is there evidence to suggest that abnormal pore pressure existed during faulting?, and finally 7. What is the structural evolution of the imbricate faults and cleavage formation? The first six questions will largely be addressed by evidence at the outcrop. The

FIGURE 3 (opposite page) Geological cross section through the pre-Silurian foreland and hinterland along a latitude of 44^0 N. The section represents the Taconian Accretionary Wedge. It is based on mapping by Cady (1945), Washington (1987), and Harding and Hartz (1987) in the foreland, by Tauvers (1982) and DelloRusso and Stanley (1986) in the Lincoln massif, and by Lapp and Stanley (1986), Prewitt (1986), Stanley (1986, 1987), Kraus (1987), Haydock (1988), Walsh (1989), Kimball-Falta (1991), and Armstrong (1993) in the Taconian part of the hinterland. North American Middle Proterozoic (Y) crust is shown by the random dash pattern. The overlying foreland rocks consist of Late Proterozoic (Z) rift clastic rocks (stippled pattern) and Cambrian and Ordovician platform rocks (carbonate and siliciclastic rocks overlain by shales) shown by the stacked rectangles. Symbols for the deformed and metamorphosed slope-rise and outer rise sequence correspond to those in Figure 1. The sequence designations are those used in Stanley and Ratcliffe (1985) and Figure 1 The black lenses in the hinterland sequence represent serpentinites. Zones 1 through 4 are based on mafic rock geochemistry (Coish, 1987, 1988). Temperatures of coexisting mineral assemblages are given as (i.e.290^0c) and are based on carbon and oxygen isotope analyses by Sheppard and Schwarcz (1970) for the foreland, oxygen isotope analyses by Garlick and Epstein (1967) and calcite-dolomite and amphibole-plagioclase temperatures (Laird and others, 1984) for the western part of the hinterland. The 471 Ma ages are based on 40Ar/39Ar analyses of hornblende by Laird and others (1984). The 376-389 Ma ages are based on 40Ar/39Ar total fusion ages of muscovite and biotite (Laird and others, 1984; Lamphere and others, 1983). The symbol a refers to amphibole, b refers to biotite, and m refers to muscovite. The metamorphic series assignment is based on amphibole analyses by Laird (1987). The solid squares represent hornblendes from the high-pressure metamorphic series and the open circles represent hornblendes from the medium-pressure metamorphic series. Based on stratigraphic and sedimentologic information, Stanley and others (1989) suggested that the root zone for the northern extension of the Taconic allochthons is located along a complex zone of pre- to late metamorphic faults that forms the western boundary of the albite-rich and aluminous rocks of the Hazens Notch, eastern Underhill and Mt. Abraham formations. This location is supported by the fact that the metabasalts in the Taconic allochthons are chemically more similar to the mafic rocks of the western Underhill and Pinnacle formations (Zone 2) than they are to the mafic rocks to the east in Zones 3 and 4. The exposed Middle Proterozoic rocks of the Lincoln massif consist of two major anticlines in which the eastern one has been severely flattened by numerous thrust faults which contain Paleozoic mylonites with east-over-west fabrics. A third anticline is buried beneath the platform sequence to the west of the East Middlebury thrust (Harding and Hartz, 1987). The breakthrough faults (East Middlebury thrust) and geometry of the western anticline suggests that the three anticlines of Middle Proterozoic rocks began their development as fault-propagation folds (Suppe, 1985). The eastern antcline was then flattened by the development of axial-surface cleavage and extensive high-angle faults. The available PT information suggests that this deformation in the massif occurred over temperatures that ranged from 290^0C to the west to 435^0 C along the eastern border of the massif. These temperatures would correspond to pressures in the range of 3 kbars (10 km) to the west and 4.5 to 5.0 kbars (16 to 18 km) to the east assuming a standard geothermal gradient of 20^0C to 30^0C per kilometer (Strehle and Stanley, 1986, Fig. 5). This information again suggests that there was a significant tectonic load over the Lincoln massif when these structures formed. The minor imbricate faults of the Middlebury synclinorium are based on work by Washington (1987). The slice of North American crust floored by the Vergennes thrust is an interpretation based on some unpublished seismic reflection work. Shortening across this section is estimated to be between 400-500 km. of which approximately 70 km involved the folding and faulting of North American crust.

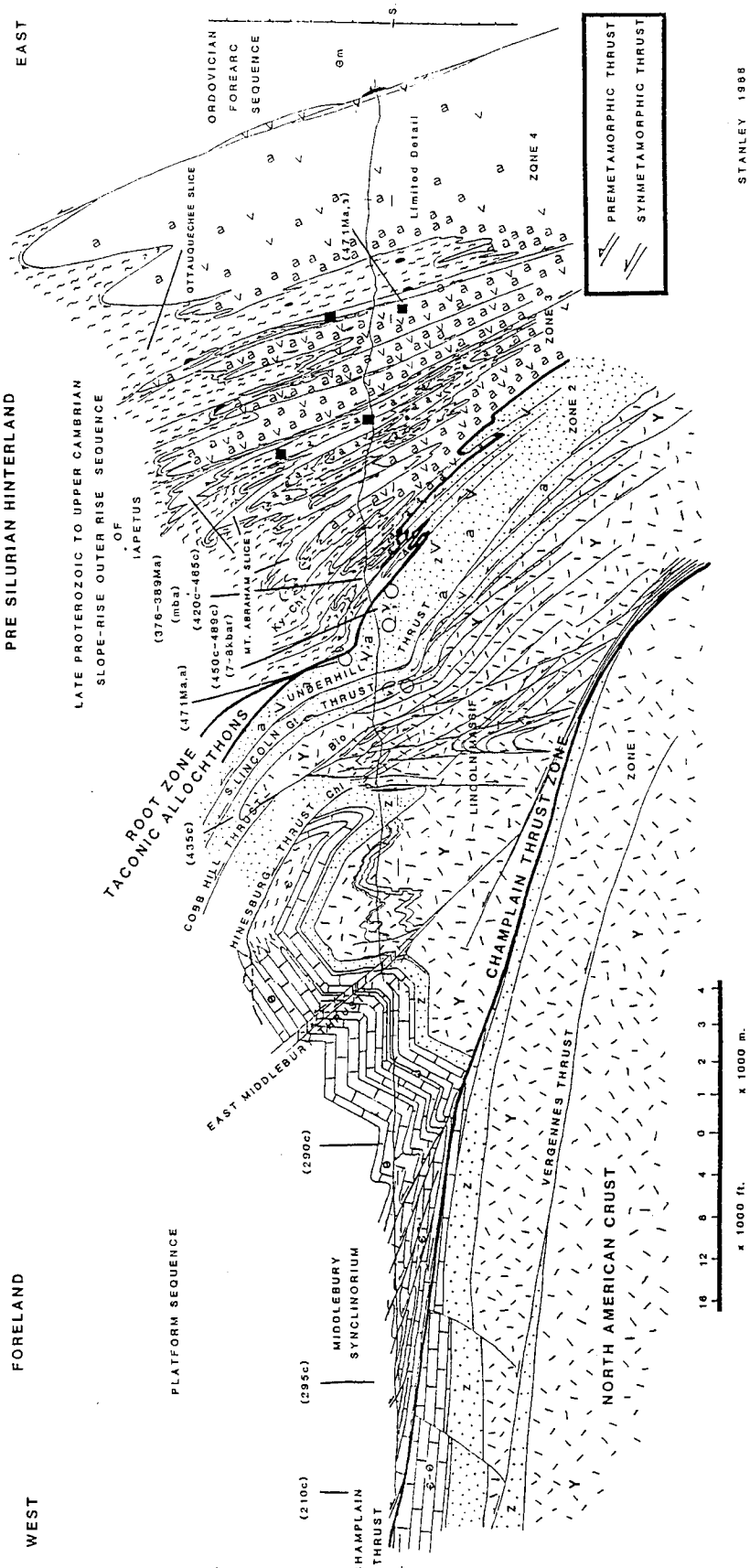
WEST
FORELAND
EAST
PRE SILURIAN HINTERLAND
PLATFORM SEQUENCE
LATE PROTEROZOIC TO UPPER CAMBRIAN
SLOPE-RISE OUTER RISE SEQUENCE
OF
IAPETUS
ORDOVICIAN
FOREARC
SEQUENCE
OTTAUQUECHEE SLICE
MT. ABRAHAM SLICE
ROOT ZONE
TACONIC ALLOCHTHONS
COSS HILL THRUST
SLINCOLN GL. THRUST
JUNBERHILL THRUST
HINESBURG THRUST
EAST MIDDLEBURY THRUST
CHAMPLAIN THRUST ZONE
VERGENNES THRUST
MIDDLEBURY
SYNCLINORIUM
CHAMPLAIN
THRUST
NORTH AMERICAN CRUST
ZONE 1
ZONE 2
ZONE 3
ZONE 4
Limited Detail
PREMETAMORPHIC THRUST
SYNMETAMORPHIC THRUST
STANLEY 1988
SCALE
x 1000 ft.
x 1000 m.

FIGURE 3

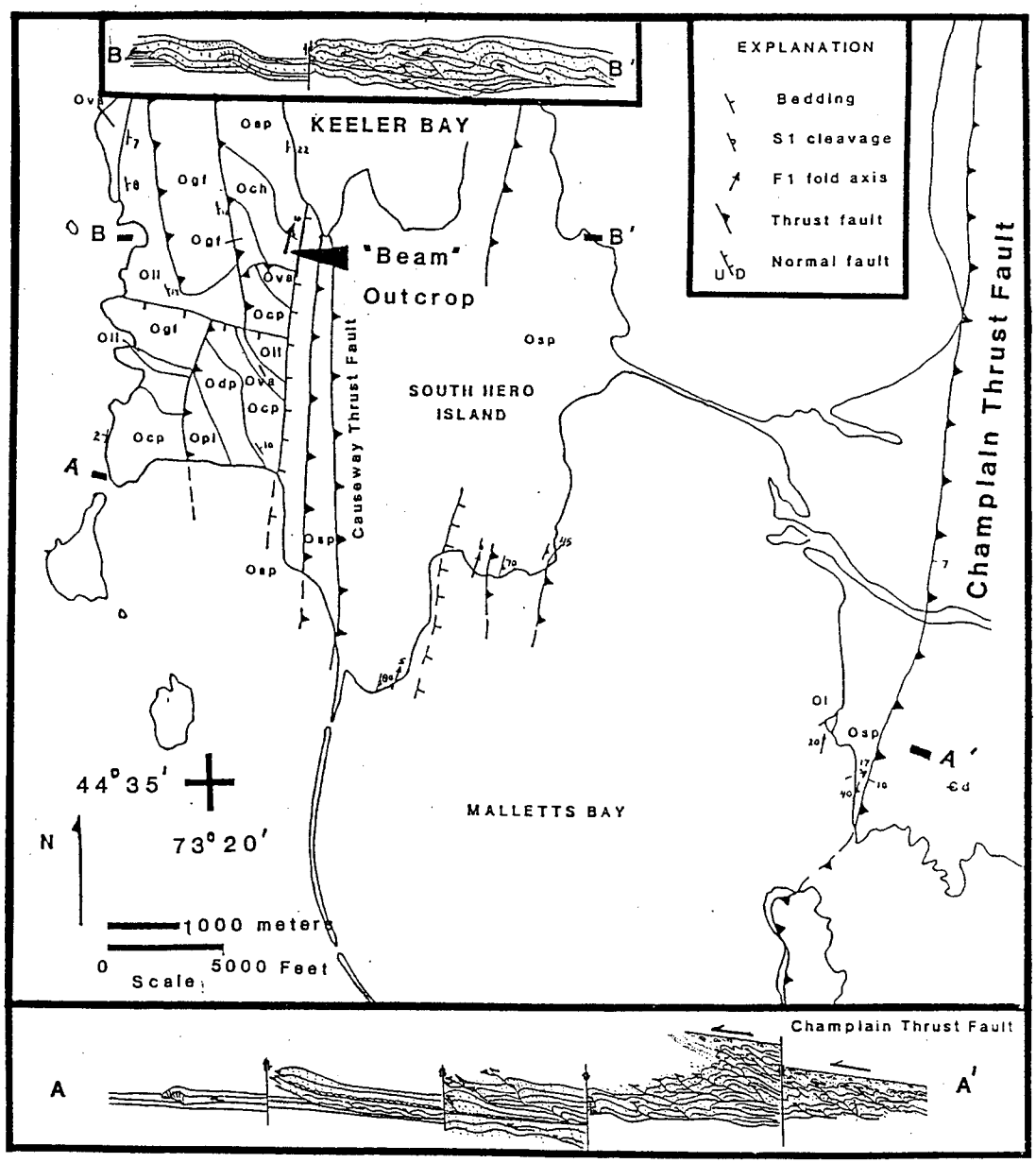

FIGURE 4 Geologic map and cross sections of the southern part of South Hero Island and eastern shore of Lake Champlain in the vicinity of Malletts Bay, Vermont. Geology by K. Leonard, 1985. Stops 1 and 2 ("The Beam") are along cross section B-B'.

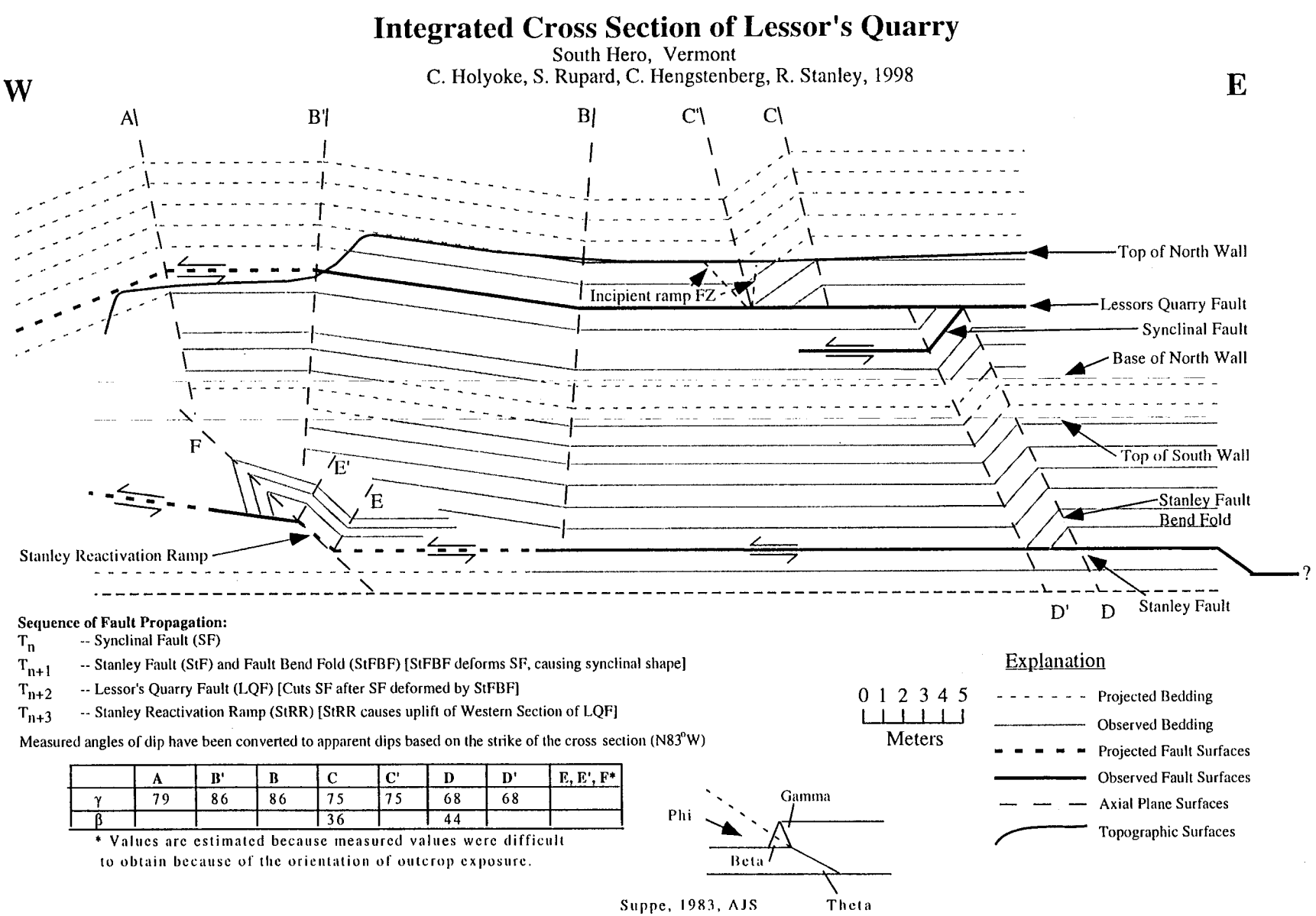

	A	B'	B	C	C'	D	D'	E, E', F*
γ	79	86	86	75	75	68	68	
β				36		44		

FIGURE 5 Integrated Cross Section of Lessor's Quarry showing a blind thrust (synclinal fault), an out-of-sequence thrust (Lessor's Quarry fault), fault-bend folds (mode 1 and 2 of Suppe, 1983). Pressure solution cleavage is not shown. These structures are considered to be representative of the Vermont foreland.

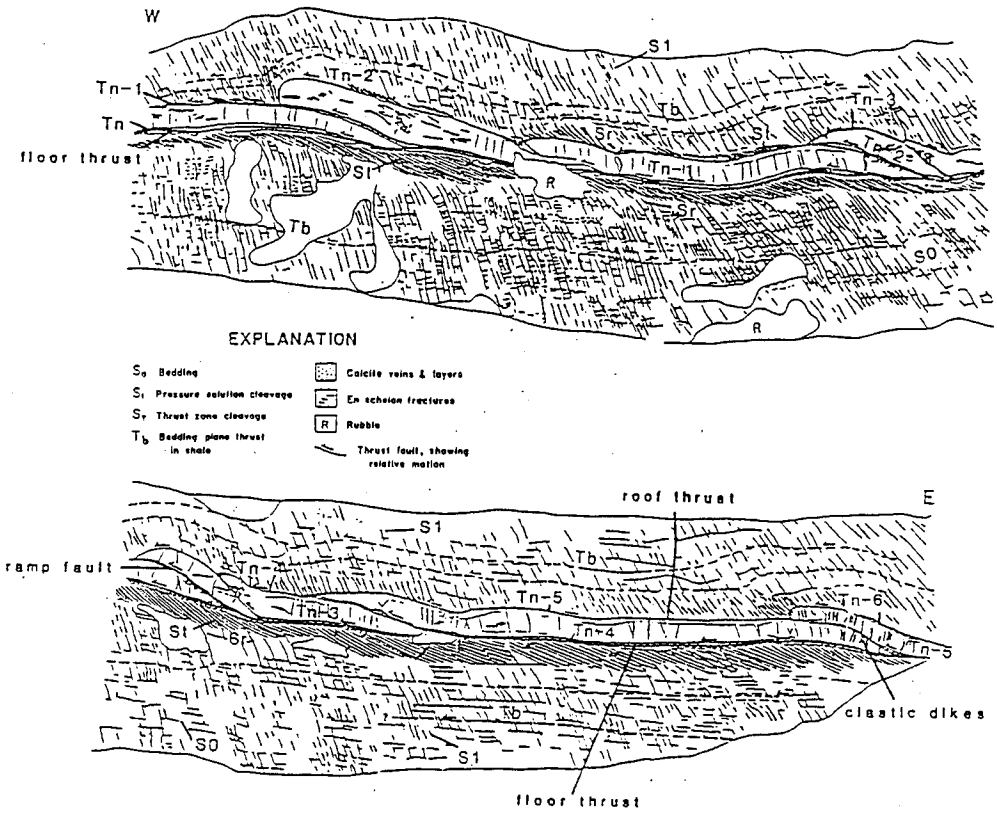

FIGURE 6a

DEFORMATION OF THE CUMBERLAND HEAD FORMATION

SOUTH HERO, VERMONT

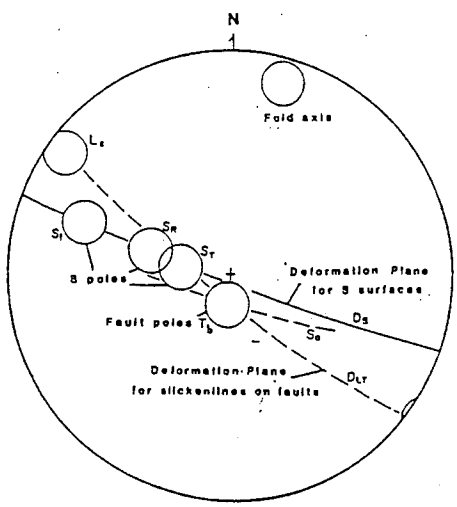

FIGURE 6b Lower hemisphere equal area projection showing the dominant position of the major structural elements in the outcrop of the "beam". The structural elements are identified in figure 7a. **Ls** refers to the dominant orientation of slickenlines on the thrust faults. The slickenlines on the older thrust faults are rotated along the deformation plane for slickenlines

FIGURE 6 Cross section of the "beam" drafted from a mosaic of overlapping photographs. Details of this outcrop are published in **Stanley, R.S., 1990, The evolution of mesoscopic imbricate thrust faults - an example from the Vermont foreland: Journal of Structural Geology, v. 12, p. 227-242.**

seventh question will be answered by palinspastically restoring the imbricated and cleaved sequence to its undeformed state.

ISOTOPE ANALYSIS, SYSTEMS DYNAMICS AND THE "BEAM" - AN INTERLUDE

(Stanley, Abbott, Whalen, and Lini , 1996, Geol. Soc. Am. Abs for Annual Meeting, Denver, Co.p.A244)

In order to determine if the calcite in the veins was derived locally from the surrounding shales, samples of the micrite and host-rock (shale) microlithons, cleaved shale, and of sparry calcite from the younger veins and floor and ramp thrusts were analyzed for stable isotopic composition. The mean carbon and oxygen isotopic composition of the younger calcite veins is similar to that of the host rock (1.3 +/- 0.02 ‰ and -7.2 +/- 0.1 ‰, respectively) which suggests local dissolution of local matrix carbonate and precipitation as vein calcite under fairly constant temperatures. Calcite veins related to different faulting events also show similar carbon and oxygen isotopic composition, suggesting that deformation occurred at each fault under similar conditions. However, fault veins were found to be enriched in 13C relative to host rock by approximately 0.2 ‰, still indicating dominant matrix control on isotopic composition. This difference is not considered to be significant at this scale, although it may indicate a temperature difference of a degree or two between carbonate dissolution and precipitation

Proposed System Dynamics Model (Fig. 7)

The foregoing geological and isotopic evidence indicates a cycling between imbricate faulting in the micrite and pressure solution in the shale during westward progression of Taconian compression. What factors controlled deformation as dominant shortening alternated between the micrite and the shale? Evidence was presented by Stanley (1990, p. 238) for intermittent development of abnormal pore pressure . During this process the transport of calcite - rich fluids from the shale was likely controlled by hydraulic conductivity of the rocks and the dissolution rate of calcite from the shale during cleavage formation. These two parameters may well have controlled the rate and duration of faulting across the outcrop. To represent this dynamic system with the feed back between the "beam" and the shale, we used a modeling code called STELLA (ITHINK) developed by High Performance Systems Inc. (1990, 1992, 1994). The basic code is embedded in four basic icons that represent the fundamental parts of any system. The rectangular icons are **stocks** which represent integrals or accumulations of quantities over time (for example, fault zone fluid, uncleaved rock, or displacement). The arrows with values are **flows** which represent quantities per unit time or differentials (for example, movement rate, fluid outflow, or pressure solution). The circular icons or **converters** represent specific values, mathematical relations or graphs that feed data into the flows or record mathematical relations during the simulation (for example, dissolution fraction, hydraulic conductivity, or a decay constant). Most of the icons are connected by arrows that represent x to y (arrow head) dependency. These are the 4 basic tools of system thinking as originally described by Jay Forester of MIT and subsequently amplified and popularized by Barry Richmond and associates at High Performance Systems Inc. (1990, 1992). The equations that describe the relations of the model are listed in Appendix 1. Short descriptions with many of the equations document the reasoning behind specific values and describe their uncertainly. Values such as hydraulic conductivity are taken from standard references (Hardcastle et al., 1989; Anderson and Woessner, 1992; Salhotra and Nichols, 1993; Manning and Ingebritsen, 1999). We suspect that the hydraulic properties of the shale become more anisotropic with cleavage. However, since hydraulic conductivities were not measured directly for the Cumberland Head Formation, an estimate of anisotropy was used in the model. Other such values as dissolution fractions are best guesses since the pressure solution reaction rates are not well constrained. Thus the model presented here is a simplified and as yet unverifiable representation of the geological system.

Two graphs are presented that illustrate the results of two separate simulation runs for the model (Figures 7b and 7c). Figure 7b represents a simulation run over 8,000 years where the hydraulic conductivity changes from 10 -9 cm/sec to 10 -11 cm/sec during the simulation. We intended this change to represent a decrease in conductivity as more cleavage is formed in the originally uncleaved rock. Figure 7c is a similar run where the hydraulic conductivity changes from 10 -11 cm/sec to 10-9 cm/sec during the simulation time of 16,000

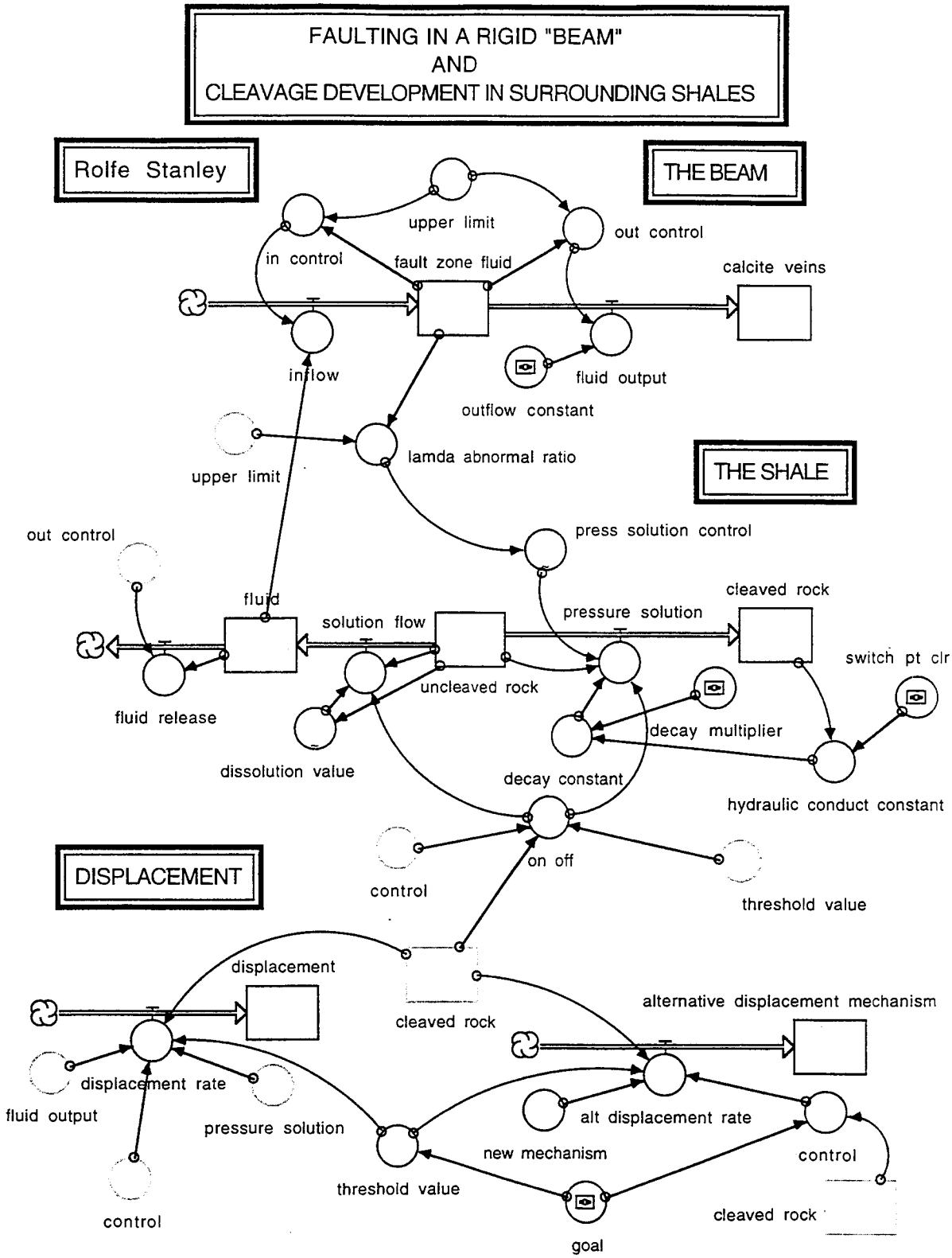

FIGURE 7A STELLA simulation model for faulting and cleavage development in the "Beam". Rectangles are **stocks**, arrows with attached circles are **flows**, isolated circles are **converters**, and arrows connecting the above elements are **connectors.** The function of the icons are explained in the text. The system is divided into 3 parts, the upper subsystem represents fluid-controlled faulting of the "beam". The middle subsystem represents the development of cleavage by pressure solution in the shale. The history of displacement is recorded in the lowest subsystem. Labels identify the geological function of the components of the system. Equations are listed in Appendix 1.

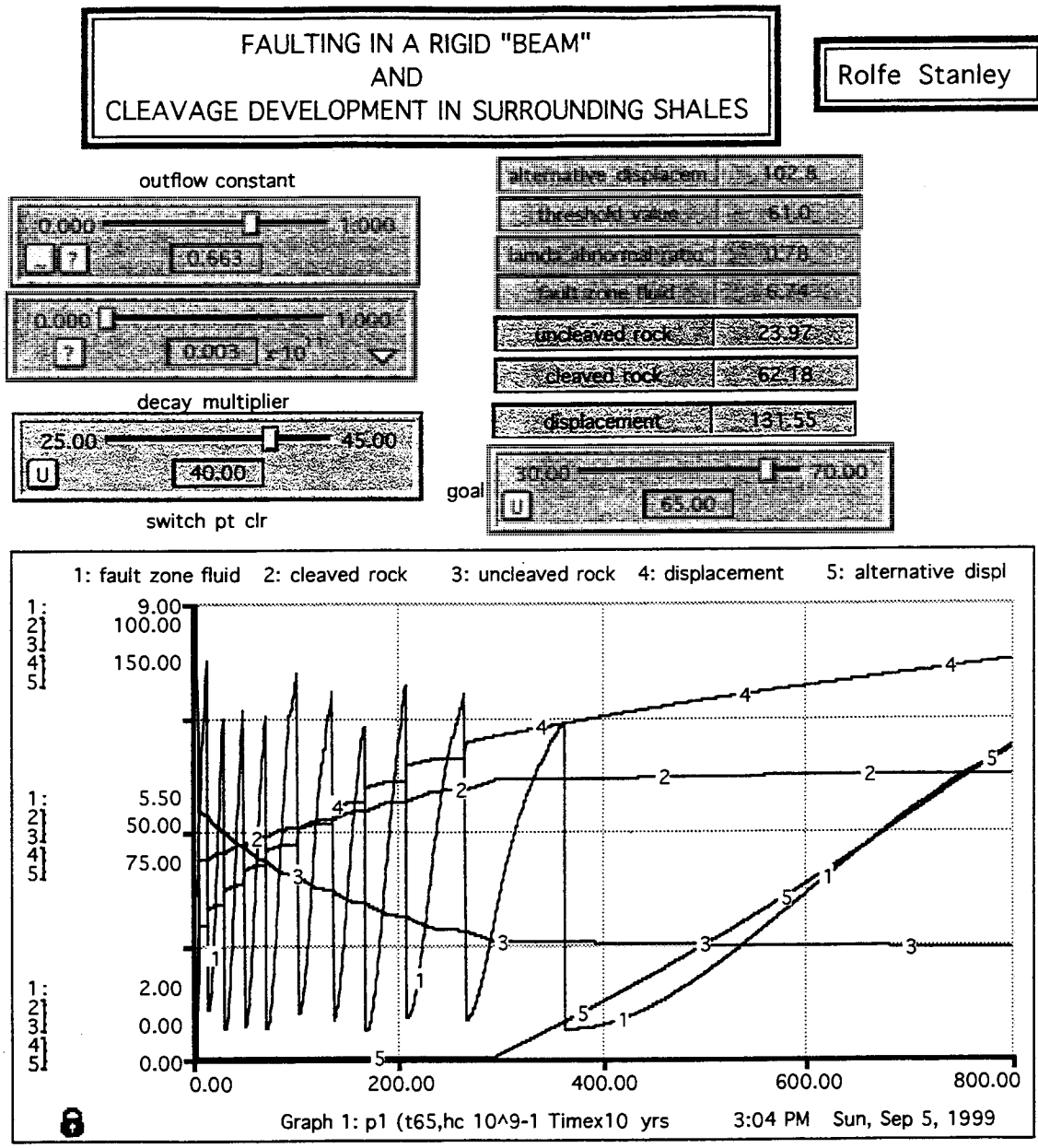

FIGURE 7B Graphical output of STELLA simulation showing the values of **fault-zone fluid** (graph 1), **cleaved rock** (graph 2), **uncleaved rock** (graph 3), **displacement** (graph 4), and **alternative displacement mechanism** (graph 5). The hydraulic conductivity begins at 10^-9 and ends at 10^-11 cm/sec. The seven thin rectangular items represent the end values for selected elements of the model. The four rectangular items with slide bars represent important model parameters (converters) set at the indicated values. The simulation represents 8000 years of evolution.

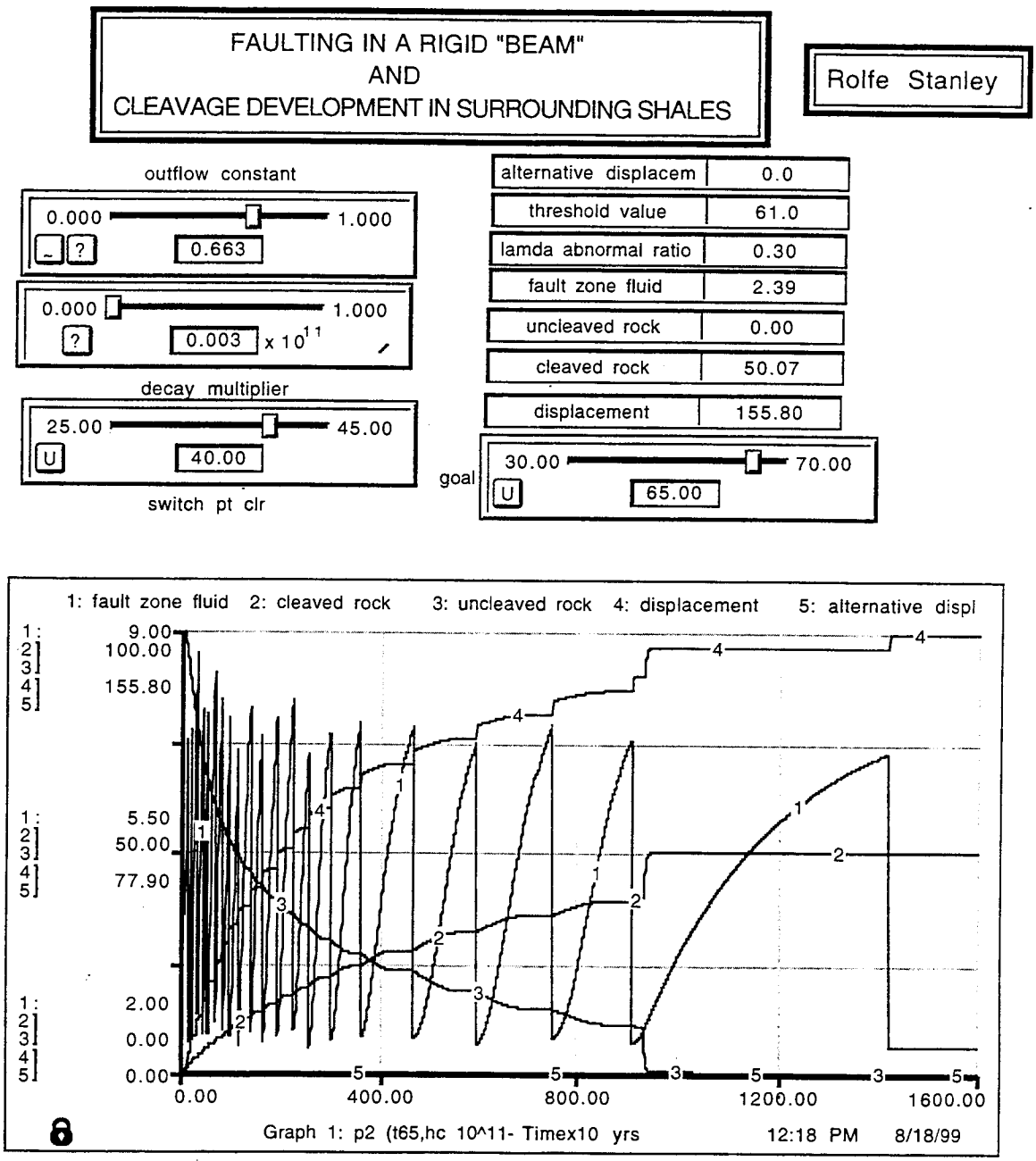

FIGURE 7C Graphical output of STELLA simulation showing the values of **fault-zone fluid** (graph 1), **cleaved rock** (graph 2), **uncleaved rock** (graph 3), **displacement** (graph 4), and **alternative displacement mechanism** (graph 5). The hydraulic conductivity begins at 10^-11 and ends at 10^-9 cm/sec. The seven thin rectangular items represent the end values for selected elements of the model. The four rectangular items with slide bars represent important model parameters (converters) set at the indicated values. The simulation represents 16000 years of evolution.

years. We intend this conductivity change to represent an increase in conductivity as more cleavage surfaces are formed during deformation. Note that the hydraulic conductivity multiplier is used to change the value of the hydraulic conductivity from cm/sec to cm/10 years. The contrast between the two graphs is striking. In the first simulation the **alternative deformation mechanism** (Fig.7a) begins at around 3,750 years (Fig. 7b). In the second simulation run over 16,000 years the **alternative deformation mechanism** part of the model (Fig. 7a) never is activated. Thus the model states that shortening continues to be accumulated by imbricate faulting and cleavage development at the "beam location" during at least 16,000 years. In both graphs, the time between faulting events, represented by the " sawtooth" curves, increases as the simulation progresses in time. This behavior represents the progressive strain hardening of the shale as more of the undeformed shale is cleaved. As the cleavage process slows down the rate of pore pressure increase also slows down thus lengthening the time between faulting events. Eventually faulting ceases since most of the uncleaved rock (98%) has been converted into cleaved rock. Thus the rock is essentially dewatered and fluid is no longer an aid in faulting. In short, the outcrop has strain hardened and further deformation has to be in the form of one or more **alternative deformation mechanism**(s) (cleavage-controlled faulting, or the development of a new cleavage, for example). Note how the graph of displacement changes during the simulation. During each faulting event the curve steepens dramatically, recording "rapid " displacement (significant faulting distance within a 10 year time step). During the intervals between fault events, the curves are gradual and represent the slow shortening by pressure solution. As time progresses during the simulation, these curved segments are more horizontal, reflecting the decreasing rate of cleavage formation as less and less undeformed shale is available. The time step used in this particular simulation represents 10 years. This value was selected so that the behavior of the subsystems for fluid-controlled faulting and pressure solution could be demonstrated within a reasonable length of computational time. Although this time step is arbitrary, we believe it may be representative of the time span of deformation since hydraulic conductivity is a very important factor in controlling fault evolution in these rocks. As a further caution, the vertical displacement on the graph that represents a "single fault

---

FIGURE 7A STELLA simulation model for faulting and cleavage development in the "Beam". Rectangles are **stocks**, arrows with attached circles are **flows**, isolated circles are **converters**, and arrows connecting the above elements are **connectors.** The function of the icons are explained in the text. The system is divided into 3 parts, the upper subsystem represents fluid-controlled faulting of the "beam". The middle subsystem represents the development of cleavage by pressure solution in the shale. The history of displacement is recorded in the lowest subsystem. Labels identify the geological function of the components of the system. Equations are listed in Appendix 1.

FIGURE 7B Graphical output of STELLA simulation showing the values of **fault-zone fluid** (graph 1), **cleaved rock** (graph 2), **uncleaved rock** (graph 3), **displacement** (graph 4), and **alternative displacement mechanism** (graph 5). The hydraulic conductivity begins at 10^-9 and ends at 10^-11 cm/sec. The seven thin rectangular items represent the end values for selected elements of the model. The four rectangular items with slide bars represent important model parameters (converters) set at the indicated values. The simulation represents 8000 years of evolution.

FIGURE 7C Graphical output of STELLA simulation showing the values of **fault-zone fluid** (graph 1), **cleaved rock** (graph 2), **uncleaved rock** (graph 3), **displacement** (graph 4), and **alternative displacement mechanism** (graph 5). The hydraulic conductivity begins at 10^-11 and ends at 10^-9 cm/sec. The seven thin rectangular items represent the end values for selected elements of the model. The four rectangular items with slide bars represent important model parameters (converters) set at the indicated values. The simulation represents 16000 years of evolution.

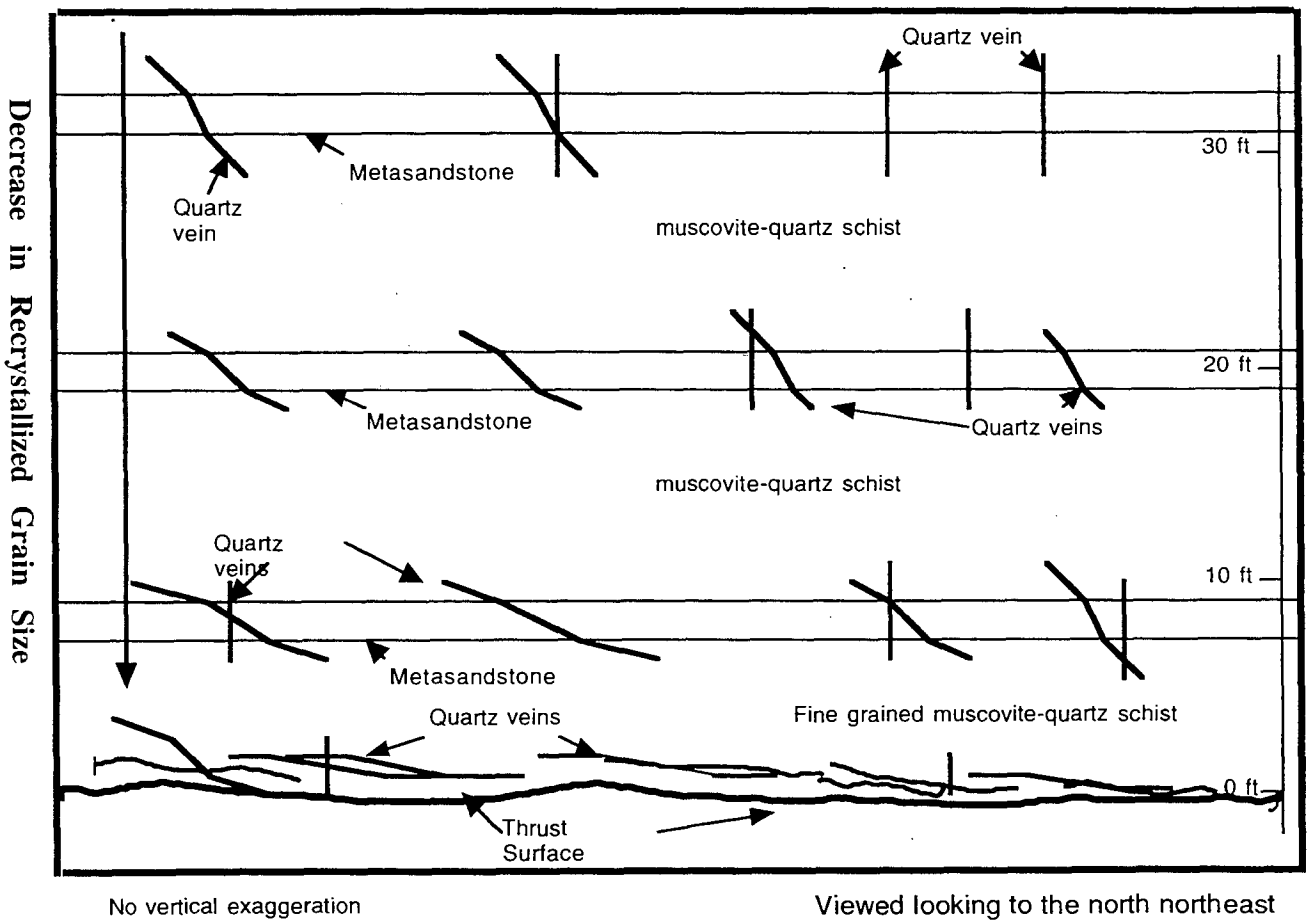

FIGURE 8 Schematic cross section of the Hinesburg thrust fault showing the distribution of superposed quartz veins in the upper plate. Adapted from the exposure at Mechanicsville just north of the village of Hinesburg, Vermont.

event" in the graphs is far too simple and must represent a whole series of small displacements or microfaulting events that result from the continual alternation between pressure solution and fault displacement. Thus the dynamic simulation is only a gross simplification of what was probably occurring during the shortening at the "beam". However, this model provides an instructive graphical representation of the long term deformation process at this outcrop.

Stop 3 HINESBURG THRUST FAULT (Fig. 8). This is the type locality of the Hinesburg thrust fault which, for central and north Vermont, is the major structural boundary between the carbonate-siliciclastic platforms of the foreland to the west and the highly deformed, and metamorphosed rift - drift sequence of the Taconian hinterland to the east. Westward displacement is in the order of 4 miles (6.4 km). Although the Lower Ordovician carbonate rocks of the lower plate are poorly exposed here, the upper plate of argillaceous quartzite of the Lower Cambrian Cheshire Formation and stratigraphic lower Fairfield Pond Phyllite form the cliffs along the western front of the hill. These rocks contain many such fault-related structures as deformed extension fractures, isoclinal folds, shear bands, mylonitic textures, slickenlines, and pressure fringes around pyrite. Many of these have been analyzed by Stanley and his students (Gillespie and others, 1972; Strehle, 1985; and Strehle and Stanley, 1986). Stanley, Martin and Smith (1993) studied the "z" shaped extension fractures. The results of this and earlier work will be discussed. We will concentrate on the following features:

1. Is the conspicuous layering in the basal part of the upper plate, bedding or foliation?
2. The presence of asymmetric fault-related folds and their relation to the Hinesburg recumbent fold.
3. The prominent mineral lineation consisting of elongate quartz and clusters of quartz grains
4. "Z" shaped quartz veins, their correlation and history throughout the upper plate.
5. Rare, east-dipping shear bands.

Return to the junction of Rt. 116 and Champlain Valley High School Road and turn south. Travel through the village of Hinesburg 16 miles (26 km) to the junction of the New Haven River and Rt. 116 just north of the village of Bristol. Turn east onto the Lincoln Gap Road. Continue east onto the Lincoln Gap Road and travel 3 miles (4.8 km) to the village of Lincoln. Continue east through Lincoln to the second bridge over the New Haven River. Park on the east side of the bridge.

Stop 4- WESTERN CONTACT OF THE EASTERN LINCOLN MASSIF (Fig. 9) This outcrop shows the western contact between the Middle Proterozoic rocks of the Eastern Lincoln massif and the overlying basal conglomerate of the Pinnacle Formation. Along most of this western boundary this contact is an erosional unconformity which dips steeply west or is slightly overturned with gentle north-plunging parasitic folds (DelloRusso and Stanley, 1986), Here, however, the contact is offset across a west-directed thrust fault (Cobb Hill thrust fault). The associated folds in the cover have been rotated toward the transport direction. The Grenvillian foliation of the Middle Proterozoic rocks is progressively overprinted by the Taconian muscovite-bearing schistosity (K/Ar age of 410 Ma on biotite, Cady 1969) of the cover as the contact is approached from the basement. The basal conglomerate of the Pinnacle is generally a quartz cobble conglomerate with minor pebbles and cobbles of granitic rocks. Here, however, large granitic cobbles and boulders form lensoidal deposits separated by quartz-feldspar metawacke. The origin of this deposit is controversial, but Stanley, following Tauvers (1982), will argue that they represent ancient channels that have been subsequently deformed into nearly reclined folds.

Continue south to where the road changes to dirt paving. Keep to the left at the junction and travel several mile south to South Lincoln where 3 roads join near several houses. The bridge to the east is the Bridge at South Lincoln where our next stop is located.

Stop 5- EASTERN CONTACT OF THE LINCOLN MASSIF (Fig. 10) - The South Lincoln thrust fault at the bridge at South Lincoln. This outcrop along the New Haven River contains a mylonitic sliver of Middle

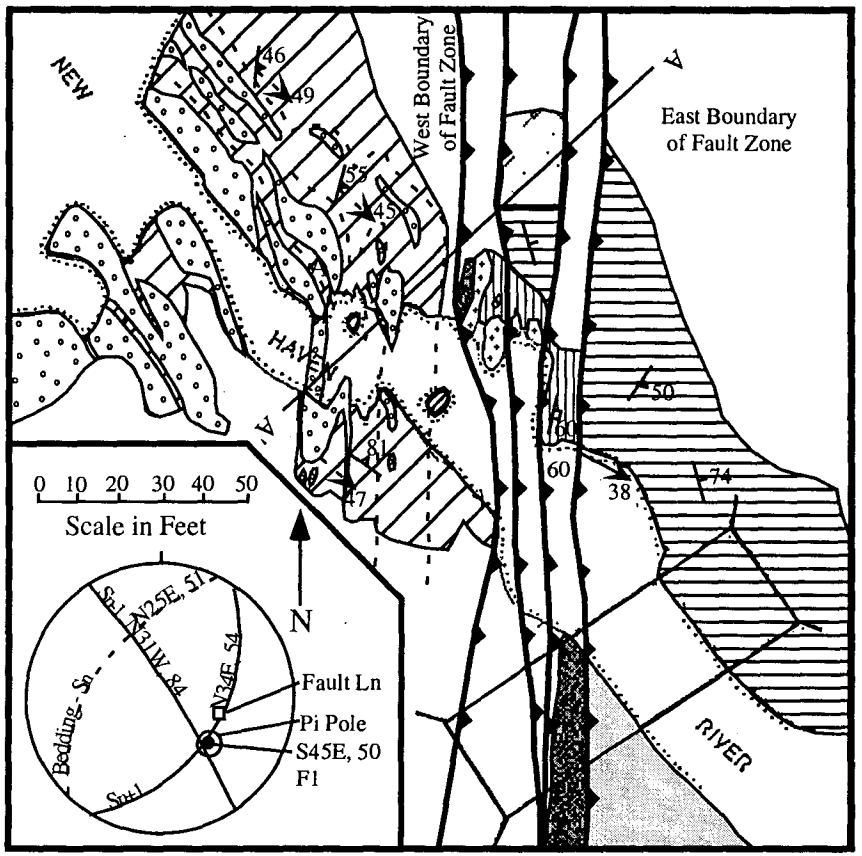

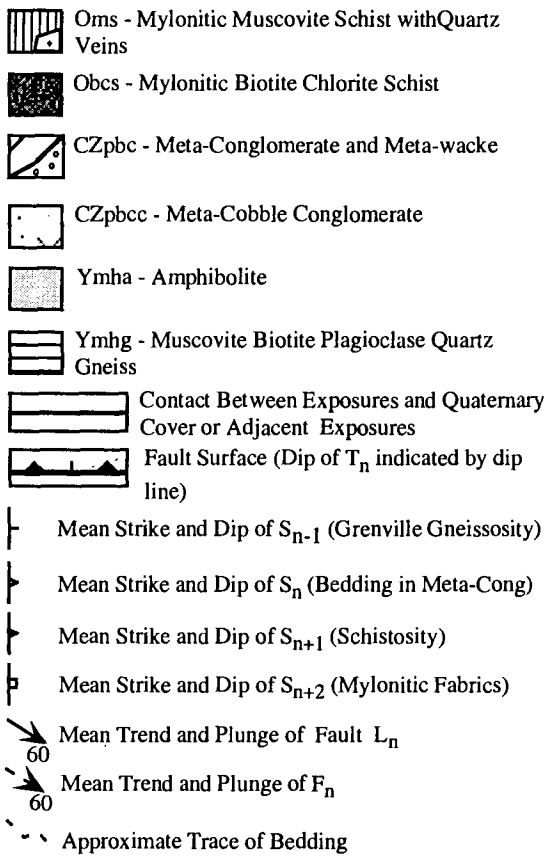

Figure 9 Geologic Map of the Cobb Hill thrust zone at Crash Bridge, Lincoln, Vermont . Mean orientations of structural measurements are on the map. The meta-cobble conglomerate located within the fault zone contains fragments of weathered gneiss. These data indicate that this unit is a saprolitic soil horizon directly adjacent to the gneiss. The metaconglomerate located to the west of the fault zone contains channel-like lenses of clast-supported conglomerate surrounded by metawacke and metaarkose. The conglomerate was possibly formed in a braided stream where velocity changed rapidly from high velocity (channel deposits) to much lower velocity between active channels where metawacke and metaarkose were formed. The Grenvillian fabric of the gneiss blocks within the fault zone is largely replaced with a muscovite-rich Taconian foliation. The mylonitic to protomylonitic schist between the gneiss blocks consist of interwoven mats of fine-grained muscovite with flattened quartz and quartz-feldspar clasts. Mappable layers of chlorite-biotite schist represent sheared Middle Proterozoic amphibolite along the south bank of the New Haven river. The large quartz pods in the fault zone indicate the importance of quartz-rich fluids in the dynamics of the Cobb Hill thrust zone. Blank areas represent surficial cover . Geologic map modified from Tauvers, 1982 and Stanley and DelloRusso, 1985. Lower hemisphere equal area net shows representative fabric. The relationship between the counterclockwise sense of rotation of the Fn folds and the more northeasterly trend of the fault lineation suggests that the Cobb Hill thrust cuts slightly earlier parasitic folds on the west side of the Lincoln Massif. These folds have been subsequently rotated into a nearly recline orientation by motion along the thrust.

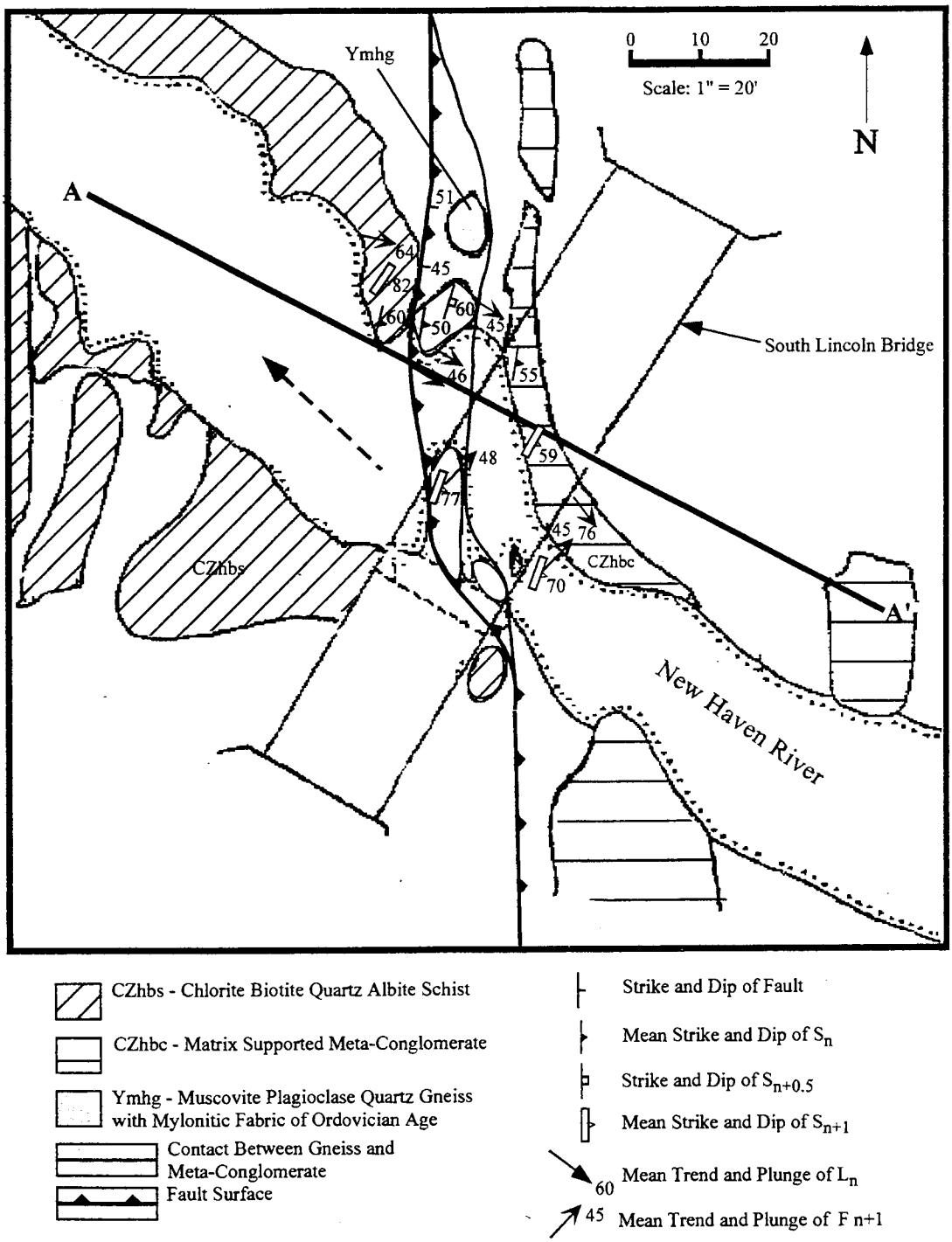

Figure 10. Geological Map of South Lincoln, Vermont. Base map taken from Tauvers (1982), but subsequently modified by DelloRusso and Stanley (1985) and Stehle and Stanley, (1986). Areas of outcrops are shaded by unit. No outcrop in blank areas. Strike and Dip measurements are means of data. A profile section looking down-plunge, perpendicular to the F_{n+1} fold axes (along section line A - A') is shown in Figure 6.

Proterozoic gneiss in thrust contact with biotite-chlorite schist of the Hoosac (Tyson) Formation. A thick conglomerate containing quartzite and granitic gneiss pebbles, cobbles, and boulders in a matrix of biotite-chlorite schist and metawacke overlies the gneiss. The clasts are identical to the Middle Proterozoic rocks in the Lincoln Massif. Late northeast-plunging folds deform the fault zone. These folds are in turn overprinted by late biotite that is randomly oriented across the dominant schistosity. Based on the fact that the feldspar in the mylonitic gneiss has been dynamically recrystallized and the surrounding rocks have been metamorphosed to the garnet grade the temperature is estimated to have been in the order of 435^0 C to 450^0 C or slightly higher (Fig. 2). These temperatures would correspond to pressures in the order of 5 to 6 kbars (17 to 20 km) (Strehle and Stanley, 1986). This synmetamorphic fault zone with a sliver of basement is typical of the eastern margin of the Lincoln massif. In fact, about 10 km. to the south fault zones like this become so numerous that they essentially make up the eastern half of the Lincoln massif as it is shown on the Geological Map of Vermont (Doll and others, 1961).

Return on the dirt road directly west of the New Haven River to the junction of the Lincoln Gap Road. Stop by the bridge that leads back to Lincoln. Do not go up the Lincoln Gap Road.

SELECTED REFERENCES

Anderson, M.P., and Woessner, W.W. 1992. Applied Groundwater Modeling: Simulation of Advective Flow and Transport: San Diego, California, Academic Press, Inc., 381 p.

DelloRusso, Vincent and Stanley, R. S., 1986, Geology of the northern part of the Lincoln massif, central Vermont: Vermont Geological Survey Special Bulletin No. 8, 35p. and 4 plates.

Doll, C.G., Cady, W.M., Thompson, J.B., and Billings, M.P., 1961, Centennial Geologic Map of Vermont: Montpelier, Vermont. Vermont Geological Survey, scale 1:250,000.

Dorsey, R.J., P.C. Agnew, C.M. Carter, E.J. Rosencrantz, and R.S. Stanley. 1893. Bedrock geology of the Milton quadrangle, Northwestern Vermont. Vermont Geological Survey Special Bulletin No. 3. 14 p. 4 pl.

Hardcastle, K.C., Wise, D.U., and Lively, G. 1989 Interim report on the relationships between lineaments, bedrock fracture fabric and well yields in the Colchester Quadrangle, Vt., University of Massachusetts.

Manning, C. E, and Ingebritsen, S. E., 1999, Permeability of the continental crust: Implications of geothermal and metamorphic systems: Review of Geophysics, v. 37, Nr. 1, American Geophysical Union, p.127-150.

McHone, J. G., 1987, Cretaceous intrusions and rift features in the Champlain Valley of Vermont: in Westerman, D. S., ed., Guidebook to field trips in Vermont, volume 2, New England Intercollegiate Geological Conference 79th Annual Meeting, p. 237-253.

Ratcliffe, N. M., Hames W. E. , and Stanley, R. S., 1998, Interpretation of ages of arc magnetism, metamorphism, and collisional tectonics in the Taconian orogen of Western New England: Am. Jour. Sci. v.298, p. 791-797.

Salhotra, A., and Nichols, E. 1993. Modeling Subsurface Contaminant Transport, Modeling Subsurface Contaminant Transport: Portland, Maine, Environmental Education Enterprises, p. 571.

Sheppard, S. M. F. and Schwarcz, H. P., 1970, Fractionation of carbon and oxygen isotopes and magnesium between coexisting metamorphic calcite and dolomite: Contributions to Mineralogy and Petrology, v. 26, p. 161-198.

Stanley, R.S., 1980, Mesozoic faults and their environmental significance in western Vermont: Vermont Geology, v. 1, p. 22-32.

----------, 1987, The Champlain thrust fault, Lone Rock Point, Burlington, Vermont: in Roy, D. C., ed., Centennial Field Guide No. 5, Geological Society of America, p. 225-228.

Stanley, R. S. and Ratcliffe, N.M., 1985, Tectonic Synthesis of the Taconian orogeny in western New England: Geological Society of America, v. 96. p. 1227-1250.

Stanley, R. S., DelloRusso, V., O'Loughlin, S. B., Lapp, E. T., Armstrong, T. R., Prewitt, J. P., Kraus, J. F, and Walsh, G. J., 1987, A transect through the pre-Silurian rocks of central Vermont: in Westerman, D. S., ed., Guidebook to field trips in Vermont, volume 2, Montpelier, Vermont, p. 272-313.

Strehle, B. A., and Stanley, R. S., 1986, A comparison of fault zone fabrics in northwestern Vermont: Vermont Geological Survey, Studies in Vermont Geology No. 3, 36 p. and 4 plates.

alternative_displacement_mechanism(t) = alternative_displacement_mechanism(t - dt) + (alt_displacement_rate) * dt
INIT alternative_displacement_mechanism = 0
INFLOWS:

alt_displacement_rate = if (cleaved_rock>=threshold_value) then (new_mechanism*1/control) else (0)
DOCUMENT: The "if , then" statements are used to turn on the flow for "alt displacement" which represents the development of alternative deformation mechanisms for the beam outcrop. These involve faulting controlled by the orientation of the cleavage which continues to benefit from cleavage formation by pressure solution although at a greatly reduced rate. As the beam outcrop strain hardens deformation most likely transgressive westward where the shales are essentially uncleaved. The "control" function results in the gradual, nonlinear development of these alternative mechanisms.

calcite_veins(t) = calcite_veins(t - dt) + (fluid_output) * dt
INIT calcite_veins = 0
INFLOWS:

fluid_output = out_control*outflow_constant
DOCUMENT: The units are fluid quantity/ time. Fluid amount should be converted into equivalent distance (cm), so that distance/time flows into displacement.

cleaved_rock(t) = cleaved_rock(t - dt) + (pressure_solution) * dt
INIT cleaved_rock = 0

DOCUMENT: cm/sec. common values for shale are 10^-7 to 10^-11 cm/sec. There are 3600 sec/hr; 86,400 secs/day; 31,536,000 sec / yr or 3.1536*10^7 sec/yr. or 3.1536*10^8sec /10 yrs or 3.2*10^9 sec/100 yrs. Because of these relations I run the time step at 1 representing a 10 year interval. If I ran the simulation at 0.5 then the time step would be a five year interval.

INFLOWS:

pressure_solution = uncleaved_rock*decay_constant*press_solution_control*on_off
DOCUMENT: Distance/time. Here cm/time. See comment for the outflow called "fluid output".

displacement(t) = displacement(t - dt) + (displacement_rate) * dt
INIT displacement = 0

DOCUMENT: Measured in cm for the beam.

INFLOWS:

displacement_rate = if (cleaved_rock<=threshold_value) then (pressure_solution+fluid_output) else (control)
DOCUMENT: distance/time or cm/time for the "beam". Need a value that converts both "fluid outflow" and "pressure solution" to a distance/time. The "if, then" statements and the "control" represent strain hardening of the shale due to dewatering and the resulting development of alternative mechanisms of deformation. The "control" allows the transition to be gradual.

fault_zone_fluid(t) = fault_zone_fluid(t - dt) + (inflow - fluid_output) * dt
INIT fault_zone_fluid = 4.5

DOCUMENT: This value can be considered to be the normal hydrostatic value that is present along a water saturated fault zone. The upper limit would the be the condition where pore pressure is equal to the load pressure. Thus the Hubbert and Rubey (1959) ratio would be 1. The initial value for this stock is 4.5 or 1/2 of the upper limit. If this stock goes below the initial value then that condition represents pore pressures below hydrostatic.

INFLOWS:

inflow = fluid*in_control
DOCUMENT: represents fluid flowing into the fault zone

OUTFLOWS:

fluid_output = out_control*outflow_constant
DOCUMENT: The units are fluid quantity/ time. Fluid amount should be converted into equivalent distance (cm), so that distance/time flows into displacement.

fluid(t) = fluid(t - dt) + (solution_flow - fluid_release) * dt
INIT fluid = 0
INFLOWS:

solution_flow = (uncleaved_rock*dissolution_value)*on_off

OUTFLOWS:

fluid_release = fluid*out_control
DOCUMENT: This outflow must be activated when faulting occurs so that fluids flow into veins near the fault zone.

uncleaved_rock(t) = uncleaved_rock(t - dt) + (- pressure_solution - solution_flow) * dt
INIT uncleaved_rock = 100

DOCUMENT: Cubic cm or cm if a constant area is divided into all volume quantities. The stock represents the quantity of uncleaved rock which is a finite resource for the outcrop of the "beam".

OUTFLOWS:

pressure_solution = uncleaved_rock*decay_constant*press_solution_control*on_off
DOCUMENT: Distance/time. Here cm/time. See comment for the outflow called "fluid output".

solution_flow = (uncleaved_rock*dissolution_value)*on_off

control = 1-(cleaved_rock)/goal

decay_constant = hydraulic_conduct_constant*decay_multiplier

decay_multiplier = 3.1536E8
DOCUMENT: Hydraulic conductivity given as cm/sec. Common values for shale are 10^-7 to 10^-11 cm/sec. There are 3600 sec/hr; 86,400 secs/day; 31,536,000 sec / yr or 3.1536*10^7 sec/yr. or 3.1536*10^8sec /10 yrs or 3.2*10^9 sec/100 yrs. This simulation is run at a value of 10^8 for the decay multiplier so that the hydraulic conductivity is given as a value of cm/10 years. Each time step is worth 10 years. A graph run for 500 time units would represent geological phenomena over 5000 years.

goal = 65

hydraulic_conduct_constant = if (cleaved_rock) <= switch_pt_clr then (10^-11) else (10^-9)
DOCUMENT: These values are the reported values for shales in cm/sec. See note under decay multiplier. The different values are intended to represent the supposed decrease in hydraulic conductivity as more of the shale is cleaved. The initial values in the "if..then" statement are 10^-9 to 10^11 which represent ranges given in the literature (see text). Sensitivity runs with different values of hydraulic conductivity" show different behavior over time of such state properties as " fault zone fluid", "cleaved rock" , "uncleaved rock", "displacement", and "alternative displacement mechanism" (compare graphs in Graph Pad 1). In general, with lower values of hydraulic conductivity (>10-9, for example), deformation by fluid-aided faulting and pressure solution is slower and the intervals between faulting events is much longer compared to higher values of hydraulic conductivity (<10^-9, for example). Thus the duration of deformation for the "beam" outcrop depends on the value of hydraulic conductivity. I also run a simulation at hydraulic conductivities that start at 10-11 and end at 10-9 simulation the possibility that the rate of fluid transport may actual increase with the development of cleavage (Manning and Ingebritsen, 1999, Reviews of Geophysics)

in_control = 1-fault_zone_fluid/upper_limit
DOCUMENT: This ratio acts as a valve that is gradually closes as the amount of fluid in the stock "fault zone fluid" increases. When the value of the stock "fault zone fluid" reaches the upper limit the inflow into the stock is zero. The upper limit represents highest value of pore pressure that can exist in the fault zone prior to actual fault motion.

lamda_abnormal_ratio = fault_zone_fluid/upper_limit

new_mechanism = .01
DOCUMENT: This number is arbitary and represents the increment in centimeters of displacement resulting from faulting along the cleavage, or movement of the deformation front westward beyond the "beam" outcrop where the rocks are essentially uncleaved. It represents any deformation processes other than fluid-added faulting of the beam or continued development of the S1 or St cleavage.

on_off = if (cleaved_rock<=threshold_value) then (1) else (control)
DOCUMENT: This statement causes faulting in the "beam" and pressure solution in the shale to stop essentially and for alternative mechanisms of displacement to begin. This is represented by the stock labeled "alternative displacment mechanisms" and the flow labeled "alt displacement rate". The threshold value is arbitary.

outflow_constant = Random(0.5,0.7,1)
DOCUMENT: Try this at 0.6, then try a graph over time, then a random function (0.5,0.7,1). What does it mean if the fault zone (stock) does not empty each time? What does the outflow constant represent in terms of the phenomena that are taking place in the fault zone ? (fracture porosity, fracture permeability)? (Read Sibson, 1975 on seismic pumping)

out_control = if fault_zone_fluid ≥ (upper_limit) then fault_zone_fluid else 0
DOCUMENT: the out control is set so that the fault actual moves at about a lamda value of .95.. thus quite high. I might actually try to set the upper limit at a random value of between 7-9. When the value of the pore pressure in the fault zone is equal to the upper limit, then lamda value approaches 1 and the resistence to movement on the fault is substantially reduced. As a result the fault moves. The system is designed to duplicate the outpouring of fluids during and just after movement on a fault.

switch_pt_clr = 35

threshold_value = goal-4
DOCUMENT: This sets the threshold value at 4 units less than the goal. The number 4 is arbitary. The threshold is the point at which the alternative deformation mechanisms begin.

upper_limit = RANDOM(7,9,1)
DOCUMENT: Random(7.0,9,1) is one selection (Taiwan value). If this is set to 10 then the volume of the fault never reaches the upper limit since the upper limit also acts as a control to the inflow. Therefore this must be set to less than 10 say 9. This relation must be placed in the outflow control (for example, upper limit-1). Because a stock can not be programmed for such "built in functions" as the randon function, I have programmed the upper limit with this random function to produce the elevated pore pressure affect.

dissolution_value = GRAPH(uncleaved_rock)
(20.0, 0.0001), (25.0, 0.0001), (30.0, 0.0005), (35.0, 0.0009), (40.0, 0.00115), (45.0, 0.0016), (50.0, 0.002), (55.0, 0.0029), (60.0, 0.0042), (65.0, 0.0053), (70.0, 0.00605), (75.0, 0.007), (80.0, 0.0075), (85.0, 0.0088), (90.0, 0.0088), (95.0, 0.0088), (100, 0.0088)
DOCUMENT: This graph represents the supposed reduction in the value of the "reaction constant" between the calcite and the adjacent clay grains. The numbers are arbitary and based on imaginary data.

press_solution_control = GRAPH(lamda_abnormal_ratio)
(0.5, 0.94), (0.533, 0.885), (0.567, 0.725), (0.6, 0.585), (0.633, 0.47), (0.667, 0.325), (0.7, 0.195), (0.733, 0.12), (0.767, 0.085), (0.8, 0.05), (0.833, 0.02), (0.867, 0.005), (0.9, 0.00)
DOCUMENT: This converter is basically a switch that activates the pressure solution process during intervals of zero fault movement.